Supplement of:

Sensitivity of snowfall radar reflectivity to maximum snowflake size and implications for snowfall retrievals

Mathias Gergely

Department of Atmospheric Sciences, University of Utah, 135 S 1460 E Room 819, Salt Lake City, Utah, USA

Contents

S1. Attached data

Sensitivities $\Delta \mathrm{dB}Z_e/\Delta D_{\max}$ of modeled snowfall radar reflectivity factors $\mathrm{dB}Z_e$ to the cutoff size $D_{\max}$ of the snowflake size distribution (SSD) are attached, calculated according to Section 2 in the main article. Each .txt file refers to one of the five analyzed snowflake representations, one of the four analyzed radar frequency bands, and one of the three analyzed SSD shape parameters μ, as indicated in the filename, and contains values of $\Delta \mathrm{dB}Z_e/\Delta D_{\max}$ in units of dB mm^{-1}, calculated at all 48 analyzed SSD slope parameters of $\Lambda = 0.3, 0.4, \ldots, 4.9, 5.0$ mm^{-1} for all 234 successive $D_{\max}$ pairs within $0.1 \leq D_{\max} \leq 23.5$ mm in steps of $\Delta D_{\max} = 0.1$ mm. A .py script is also included that allows a basic visualization of the attached sensitivity data.

S2. Additional figures

Email address: mathias.gergely@utah.edu (Mathias Gergely)

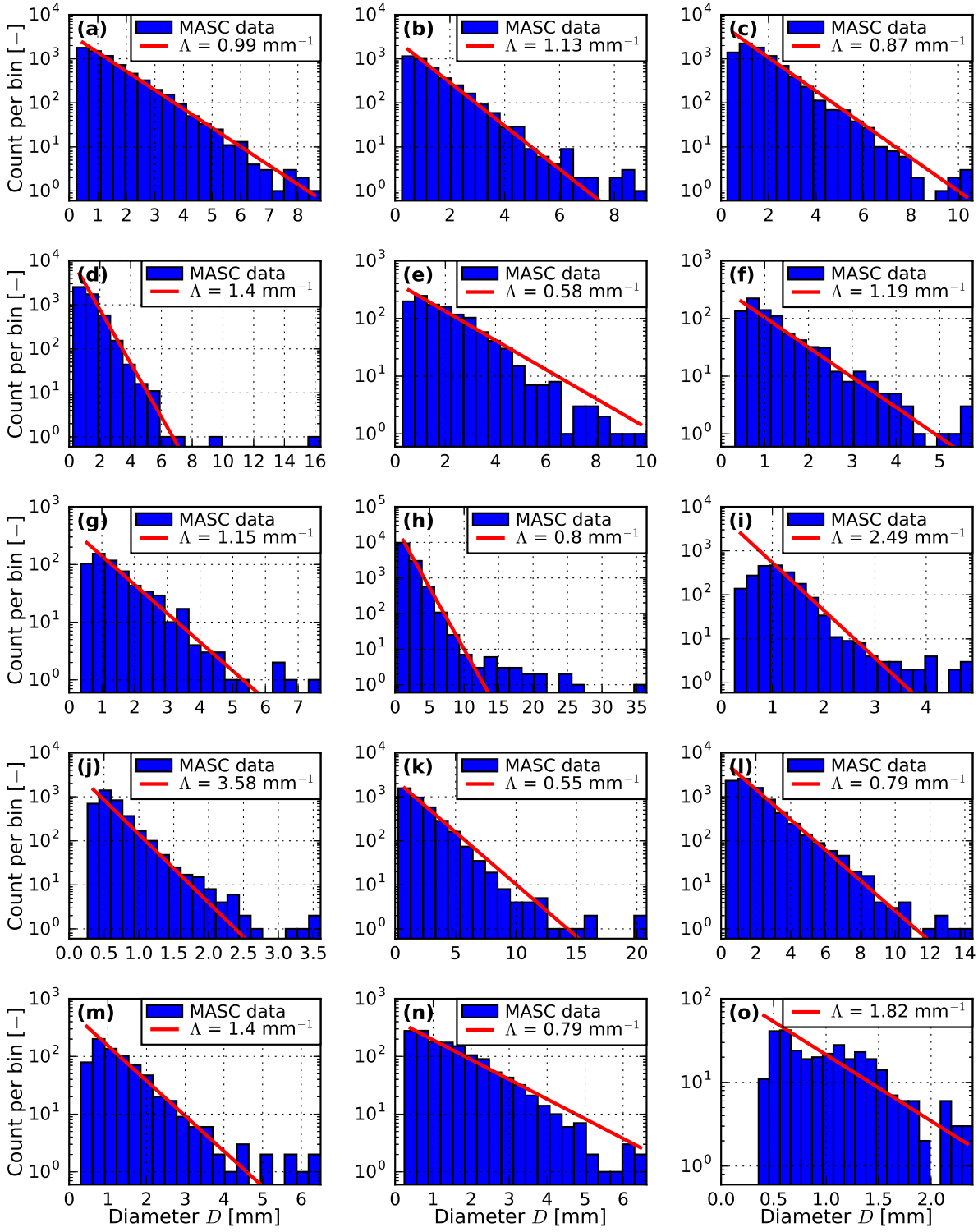

Figure S1: Examples of binned snowflake size distributions (SSDs) derived from Multi-Angle Snowflake Camera (MASC [1]) measurements at Alta and at Barrow with corresponding exponential slope parameters Λ that were determined by the nonlinear least squares method for fitting an exponential SSD to MASC data for snowflake sizes of $D > 1.0$ mm [2].

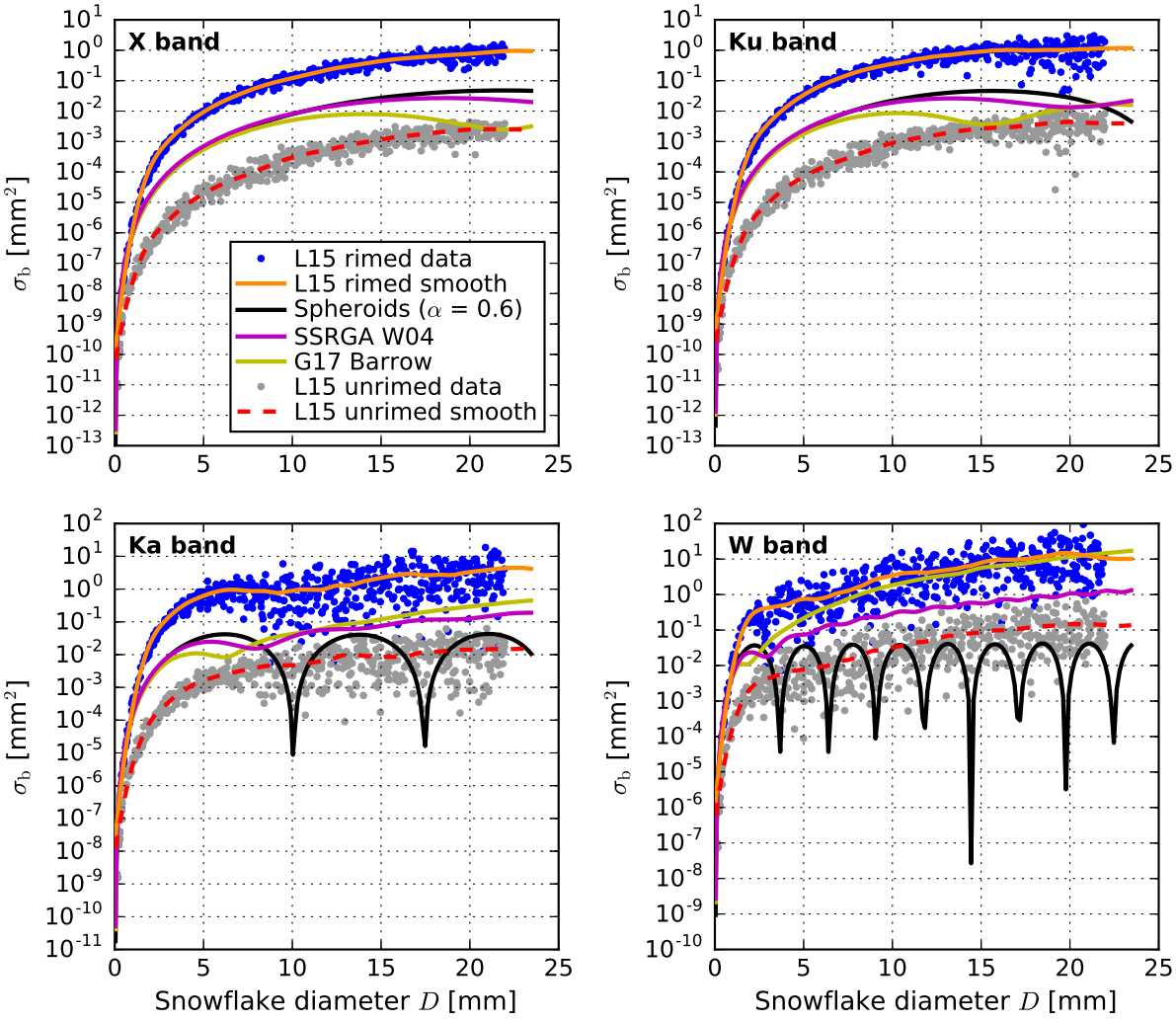

Figure S2: Overview of modeled snowflake radar backscatter cross sections σ_b for different snowflake representations used in the analysis: L15 synthetically generated rimed and unrimed snowflakes [3], horizontally oriented oblate soft spheroids with aspect ratio $\alpha = 0.6$, SSRGA W04 [4–6], G17 Barrow [2]; snowflake masses for soft spheroids, SSRGA W04 and G17 Barrow snowflake representations were derived from snowflake diameter D following a previously determined mass parameterization [7]. See Section 2.2 in the main article for details.

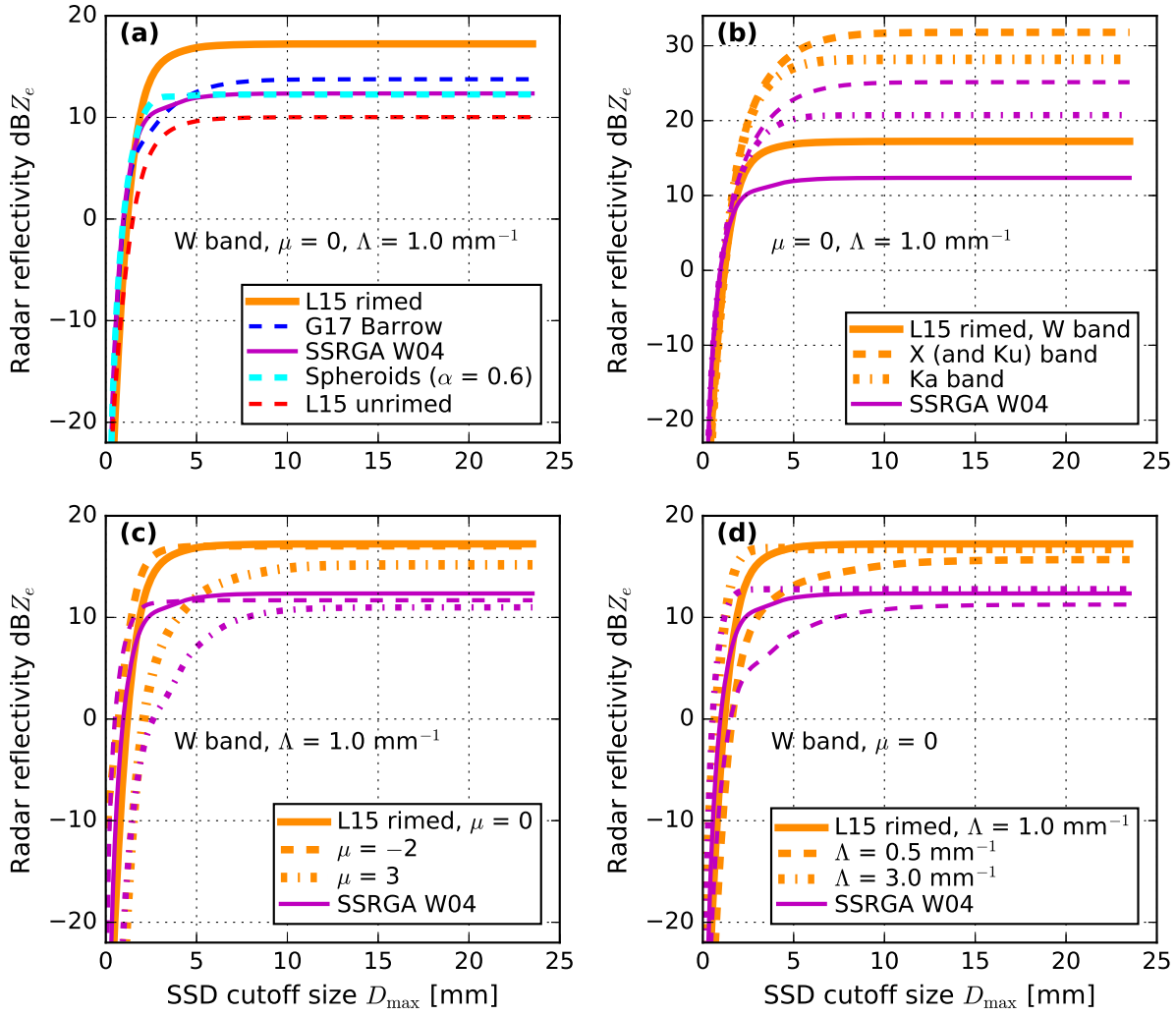

Figure S3: Modeled radar reflectivity factors dBZ_e as in Fig. 3 in the main article, but focusing on W band instead of Ku band.

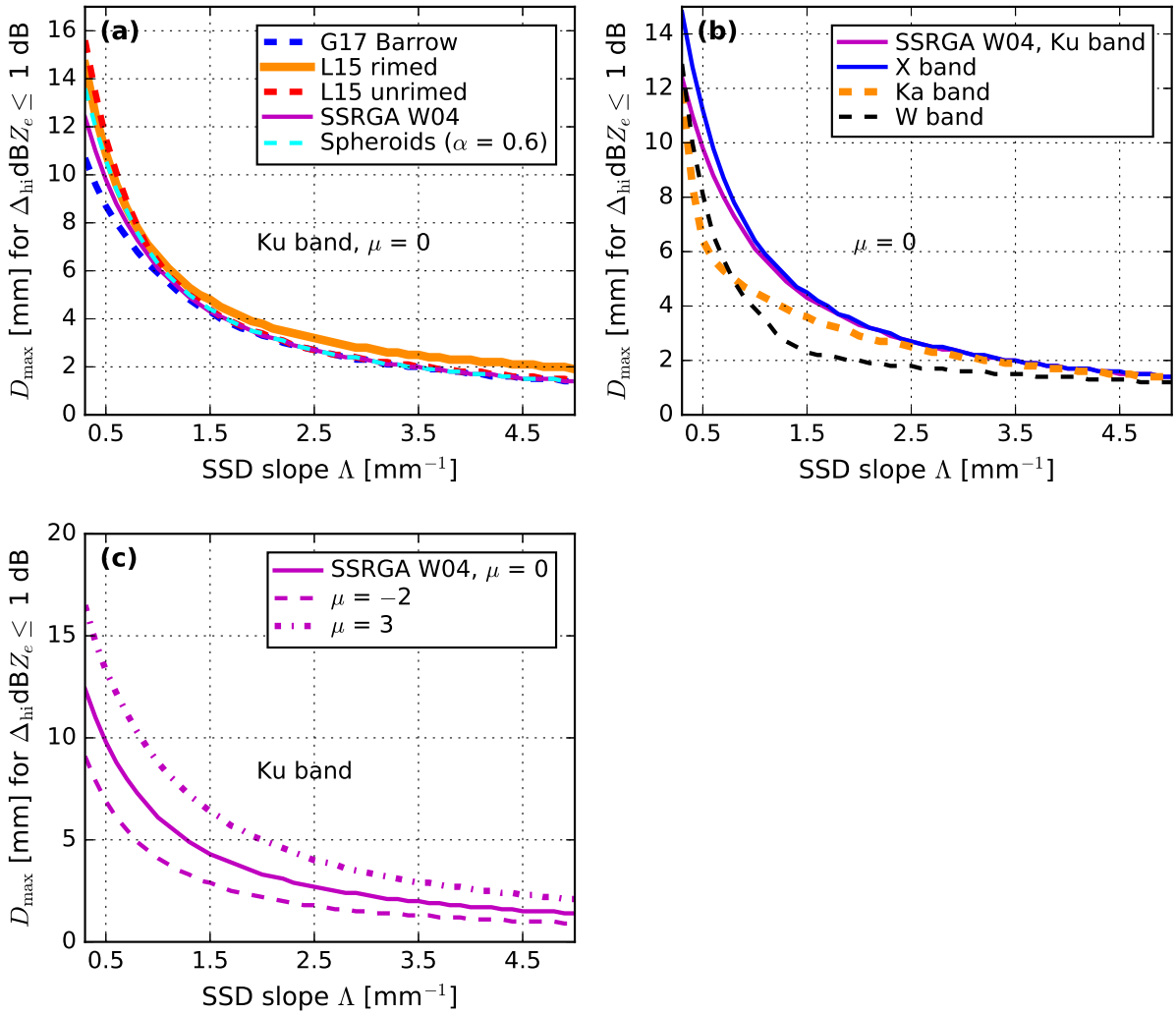

Figure S4: Lowest values of SSD cutoff size $D_{\max}$ with modeled radar reflectivity factors $\mathrm{dB}Z_e(D_{\max})$ within 1 dB of corresponding $\mathrm{dB}Z_e(D_{\max} = 23.5\ \mathrm{mm})$, with $\Delta_{\mathrm{hi}}\mathrm{dB}Z_e = \mathrm{dB}Z_e(D_{\max} = 23.5\ \mathrm{mm}) - \mathrm{dB}Z_e(D_{\max})$.

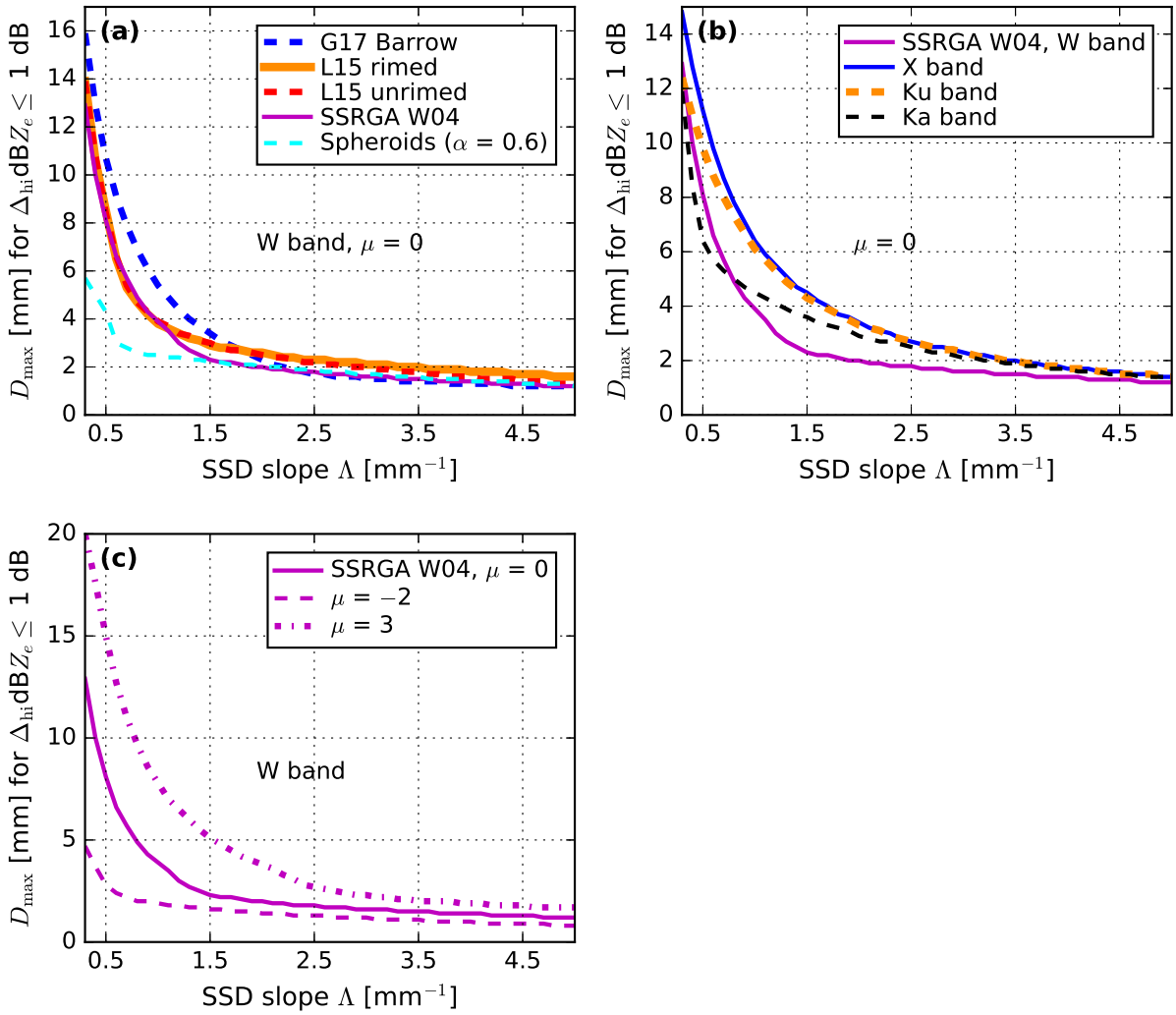

Figure S5: As Fig. S4, but focusing on W band instead of Ku band.

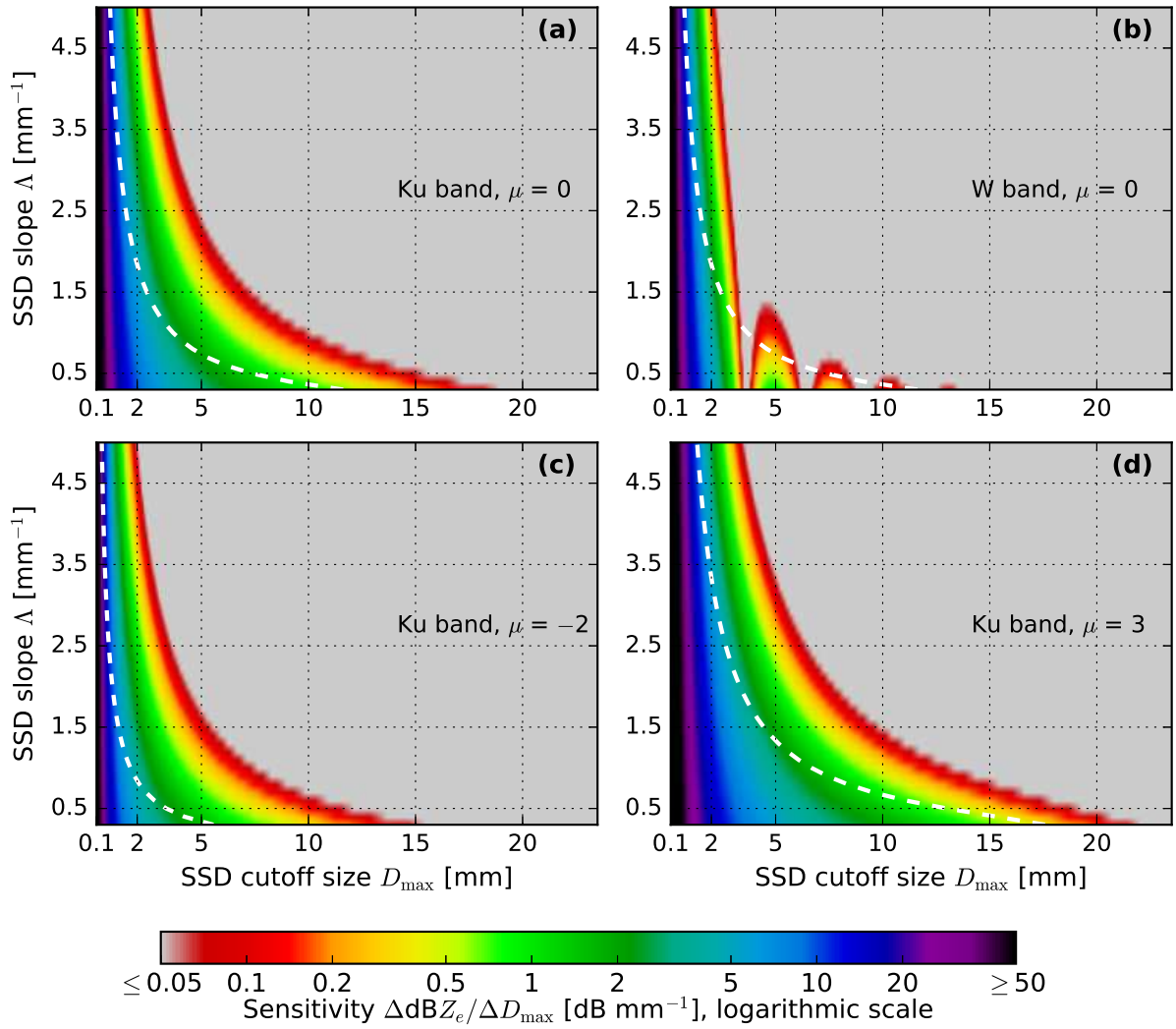

Figure S6: Sensitivity $\Delta \mathrm{dB}Z_e / \Delta D_{\max}$ of modeled snowfall radar reflectivity factors $\mathrm{dB}Z_e$ to SSD cutoff size $D_{\max}$ as in Figs. 4 and 5 in the main article, but for snowflakes represented by horizontally oriented oblate soft spheroids with aspect ratio $\alpha = 0.6$.

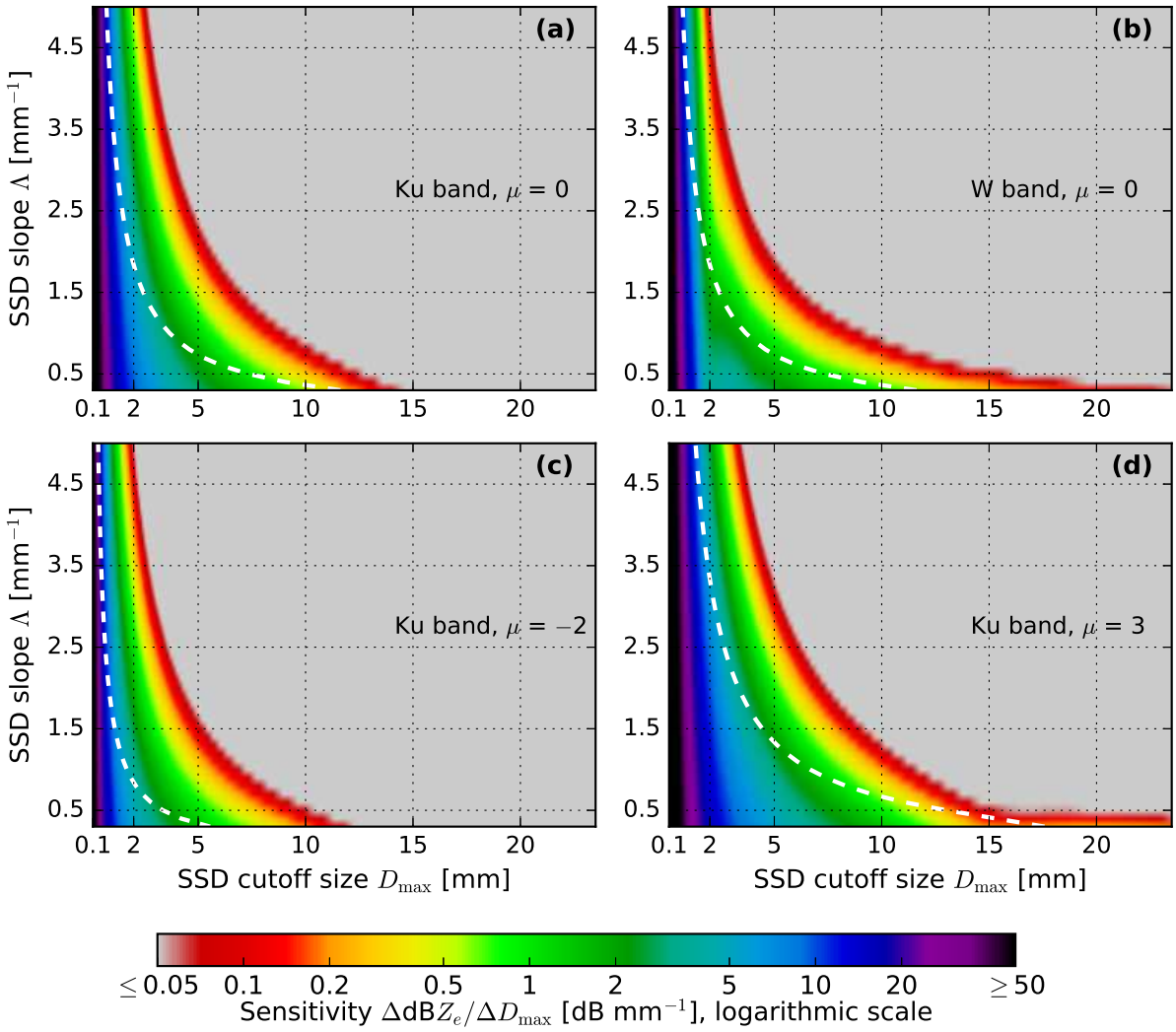

Figure S7: As Fig. S6, but for representing snowflakes according to G17 Barrow description.

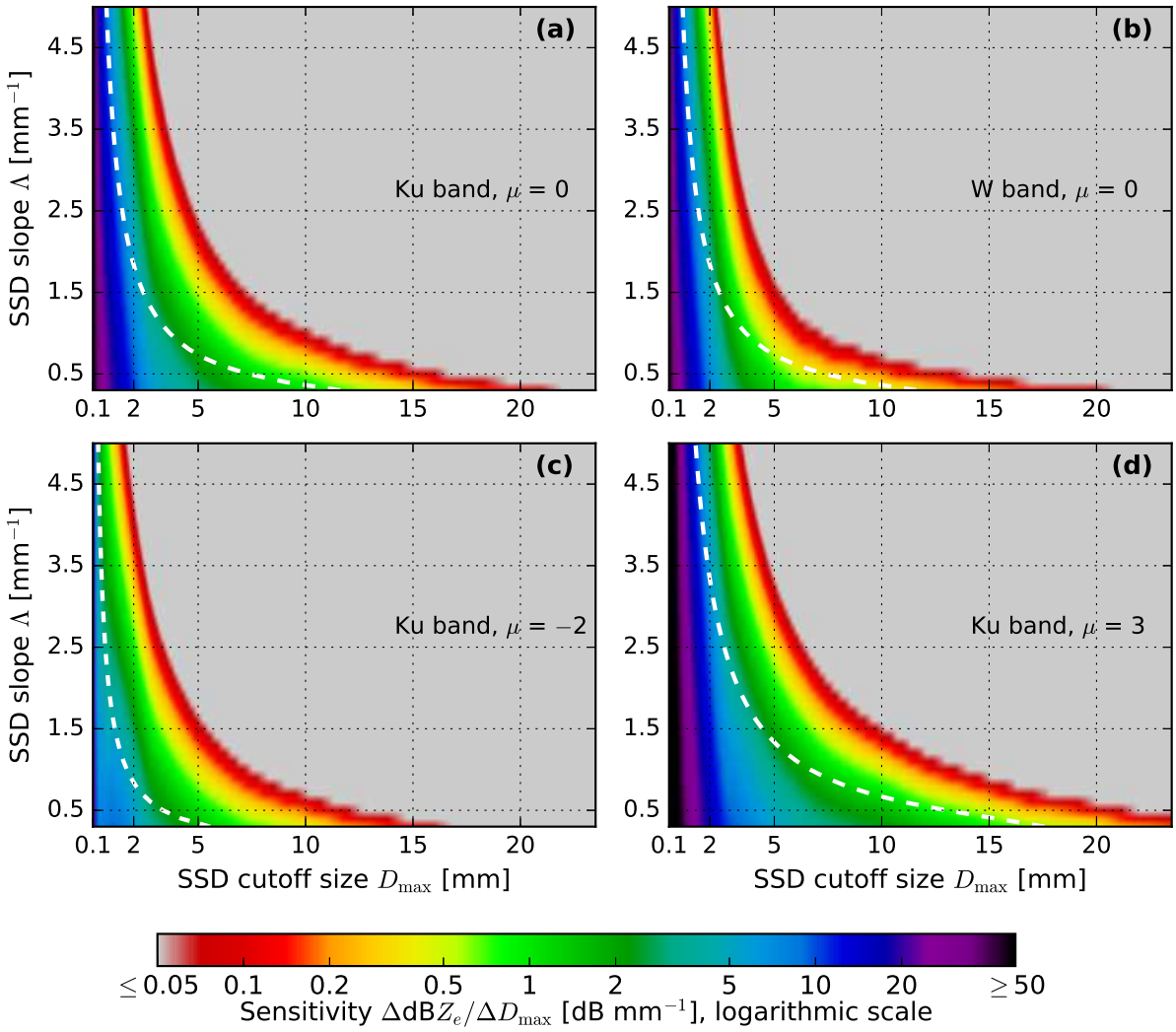

Figure S8: As Fig. S6, but for smoothed data of L15 unrimed snowflake 3-D shape models.

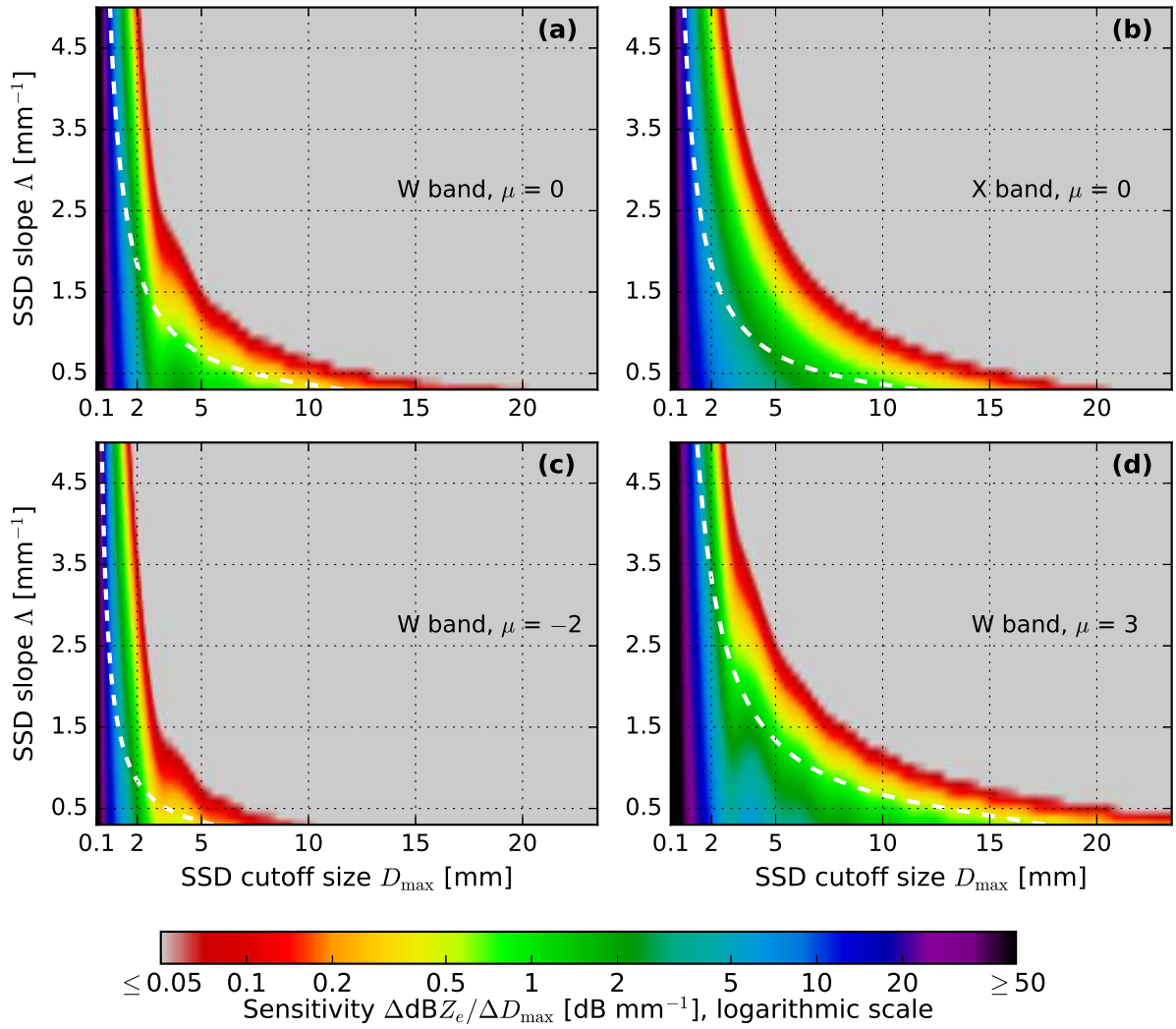

Figure S9: Sensitivity of modeled snowfall radar reflectivity factors dBZ_e to SSD cutoff size $D_{\max}$ for SSRGA W04 as in Fig. 4 in the main article, but focusing on W band instead of Ku band.

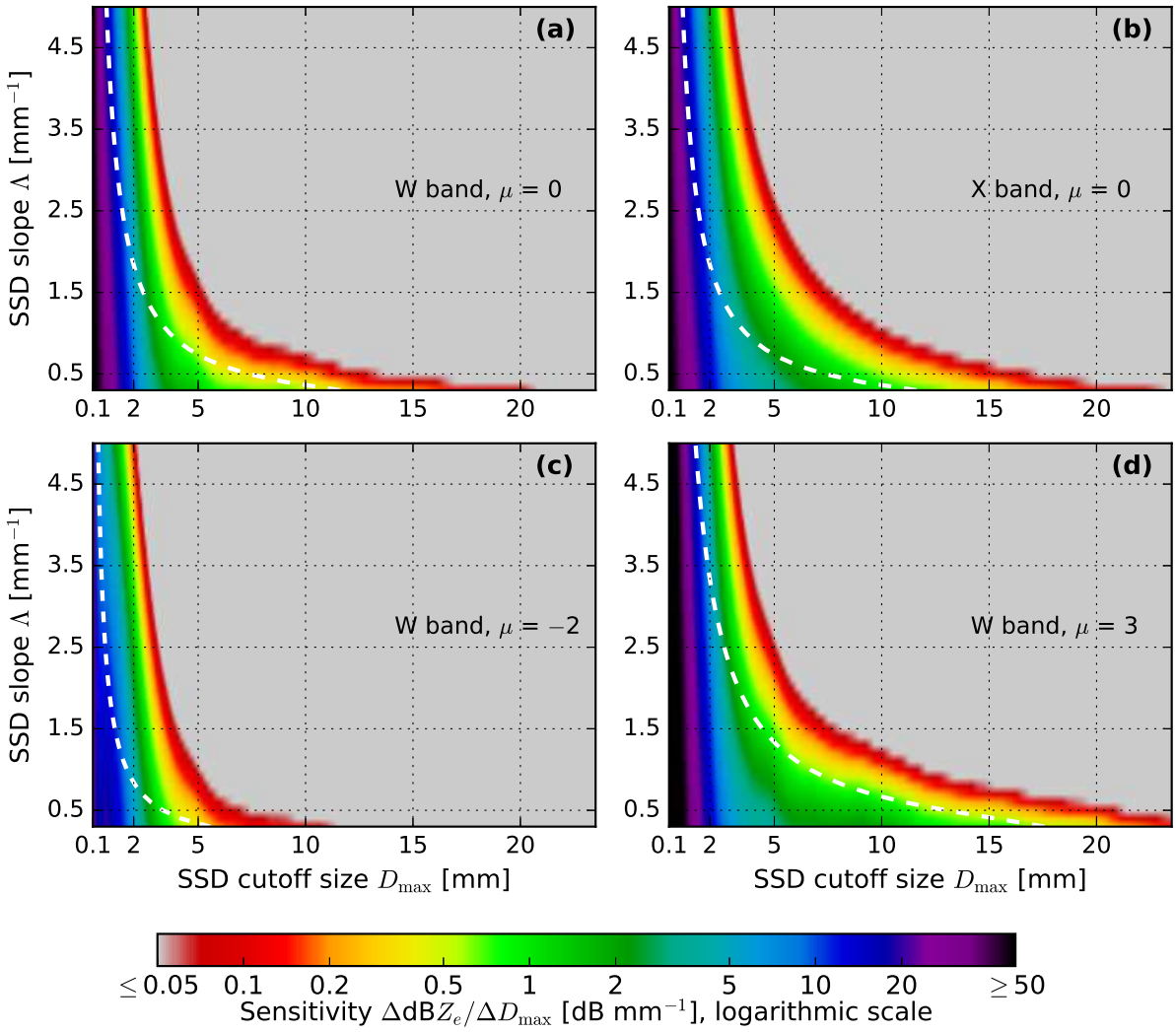

Figure S10: As Fig. S9, but for smoothed data of L15 rimed snowflake 3-D shape models.

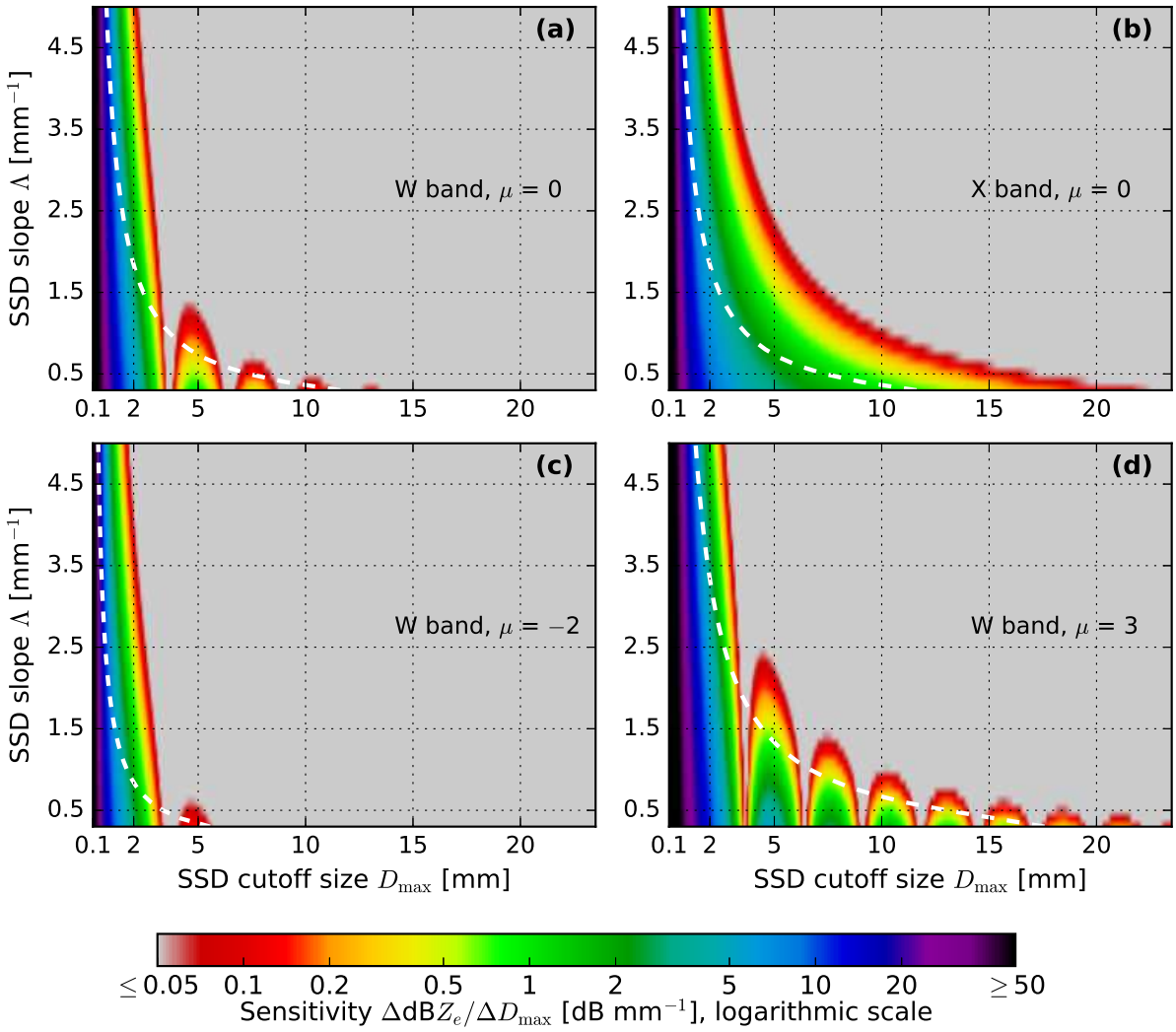

Figure S11: As Fig. S9, but for snowflakes represented by horizontally oriented oblate soft spheroids with aspect ratio $\alpha = 0.6$.

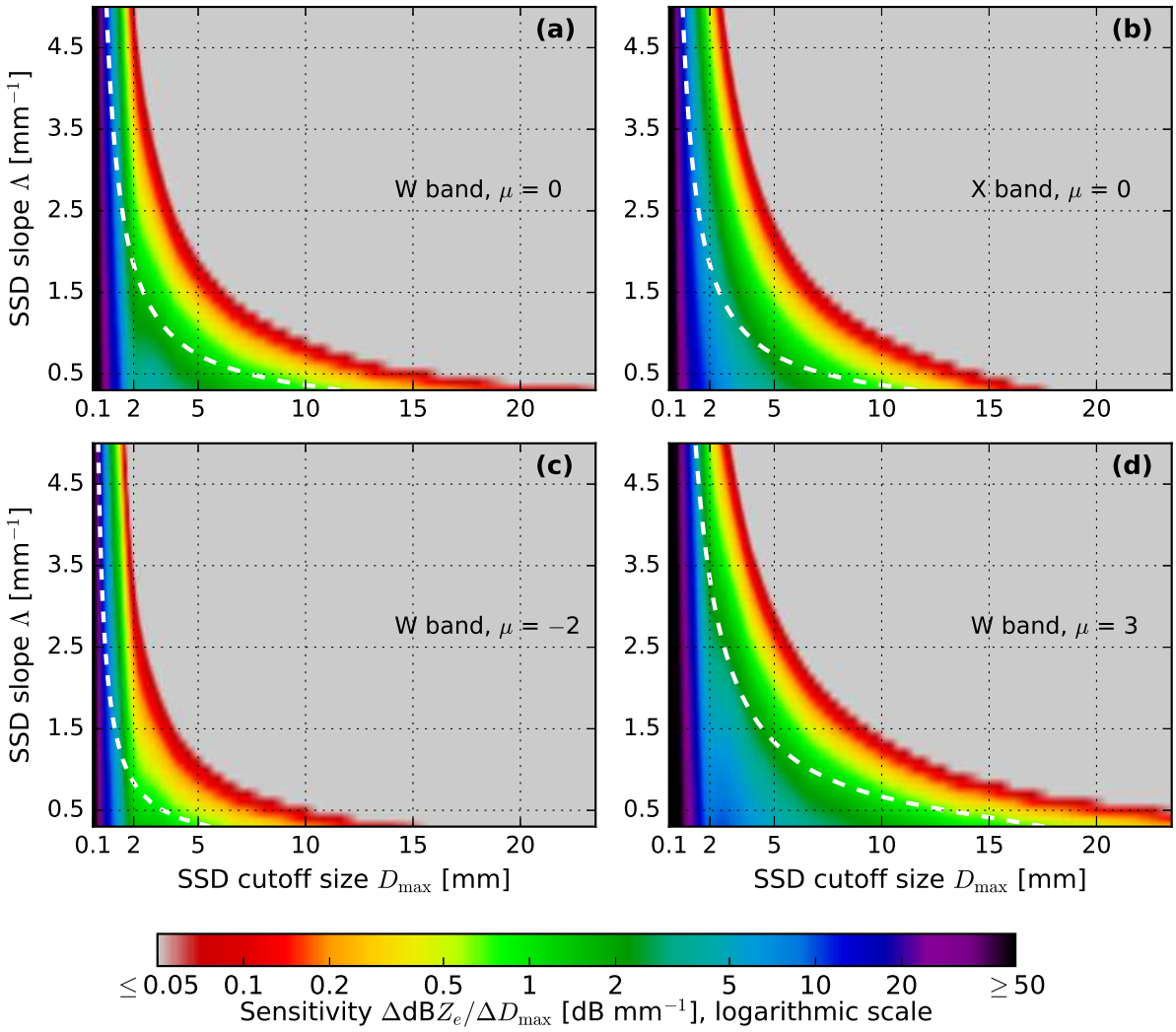

Figure S12: As Fig. S9, but for representing snowflakes according to G17 Barrow description.

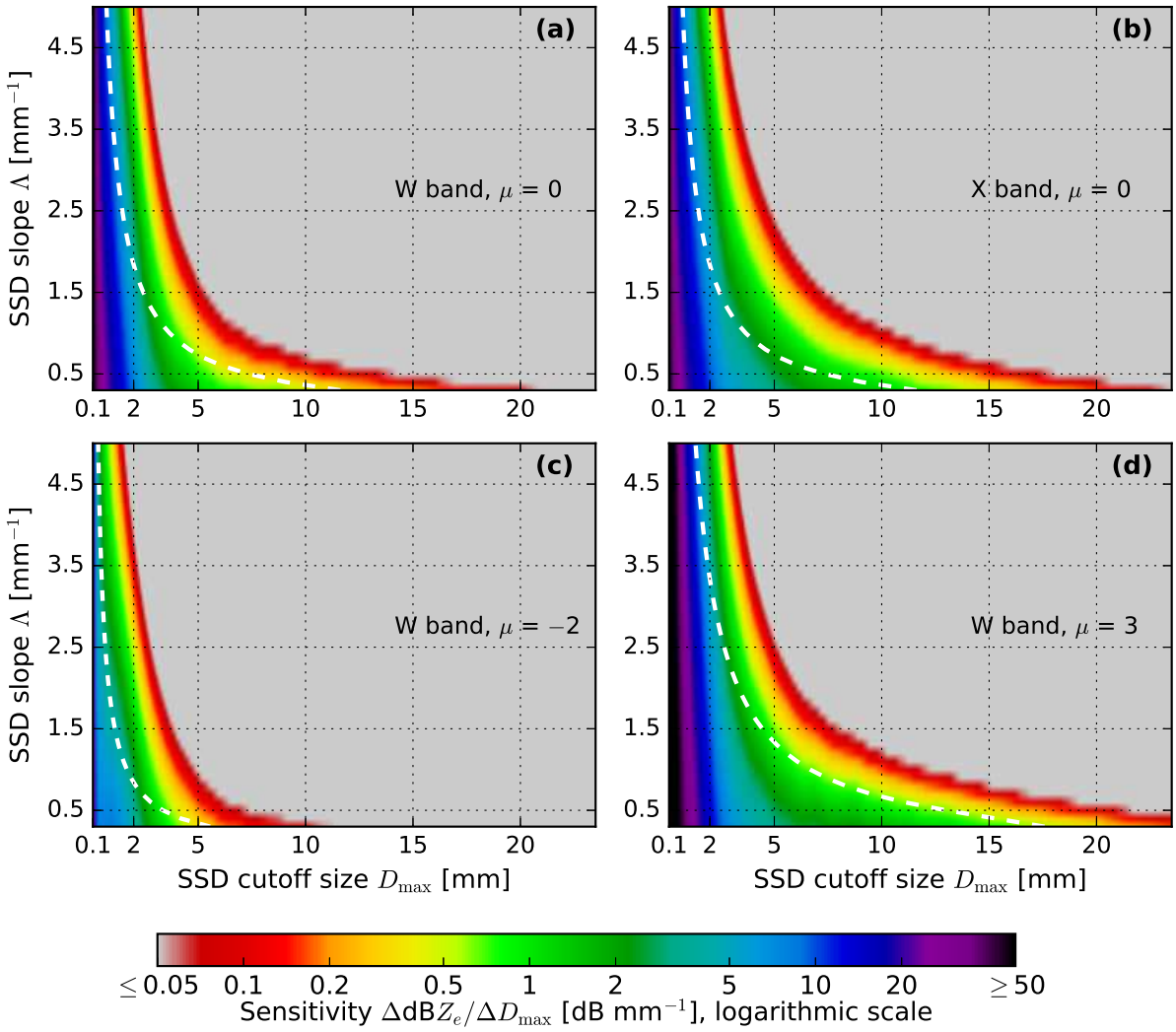

Figure S13: As Fig. S9, but for smoothed data of L15 unrimed snowflake 3-D shape models.

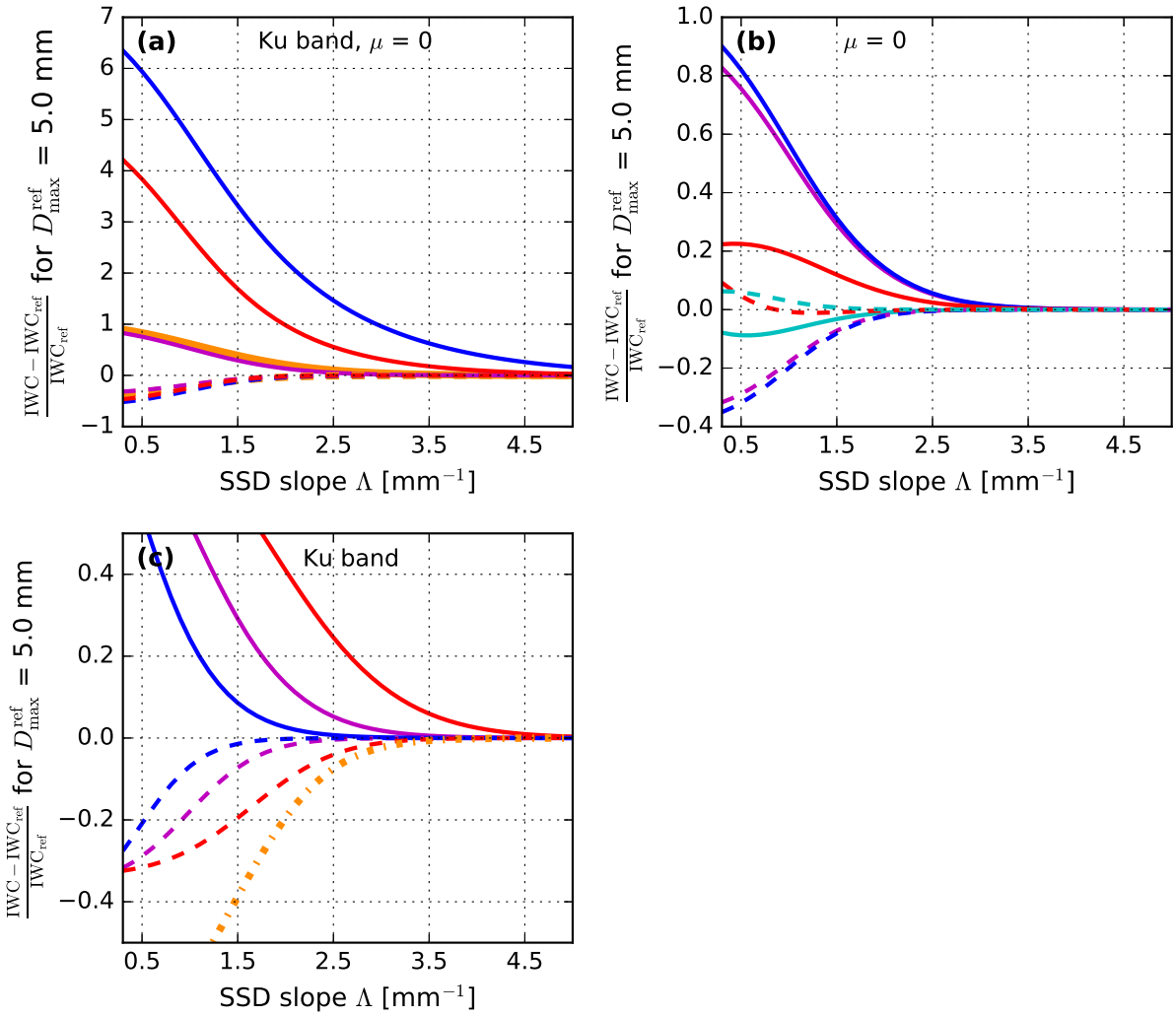

Figure S14: Impact of SSD cutoff size D_{max} on the retrieval of snowfall ice water content (IWC) as in Fig. 6 in the main article, but for a D_{max} reference value of $D_{\mathrm{max}}^{\mathrm{ref}} = 5.0$ mm.

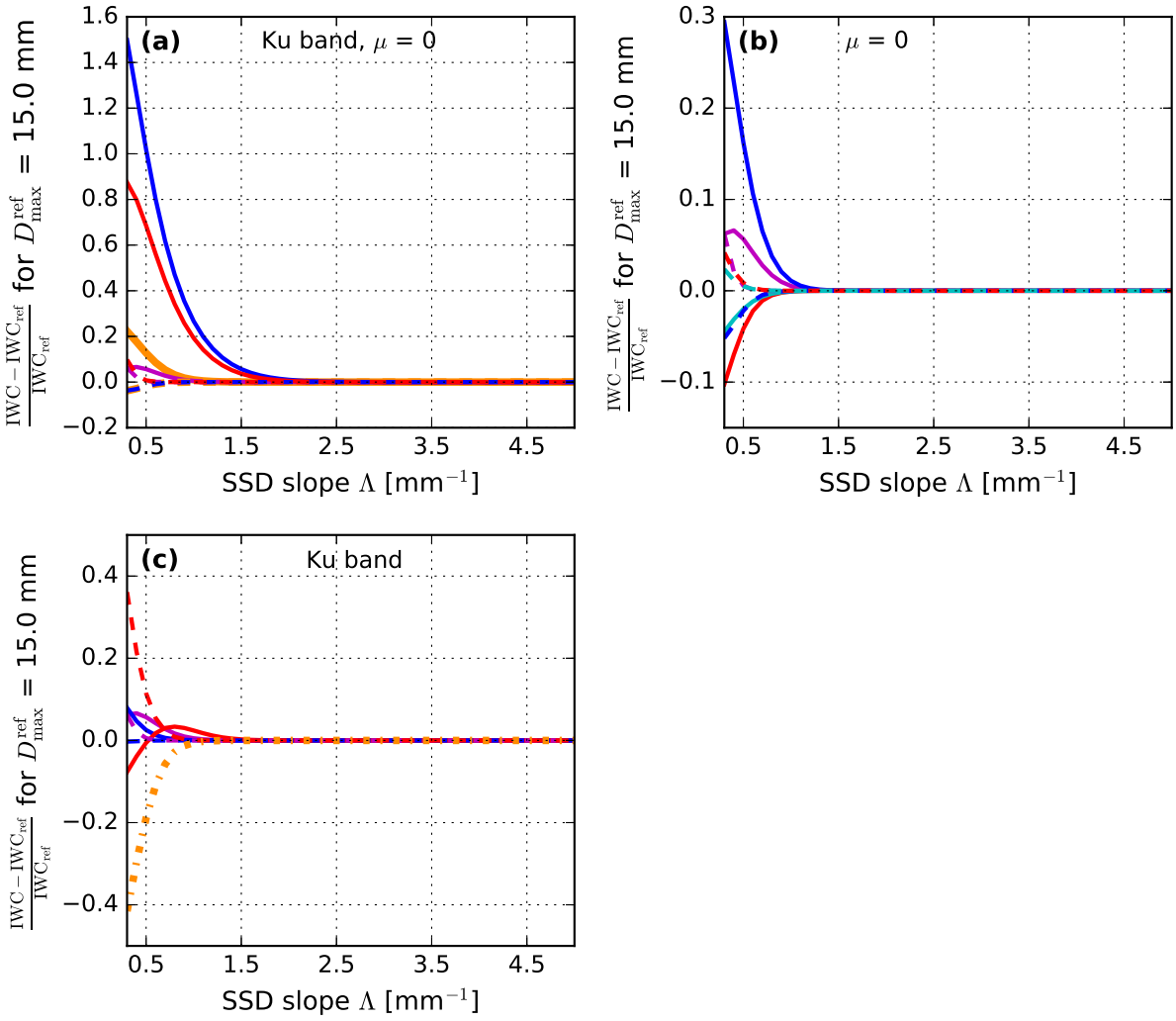

Figure S15: As Fig. S14, but for $D_{\mathrm{max}}^{\mathrm{ref}} = 15.0$ mm.

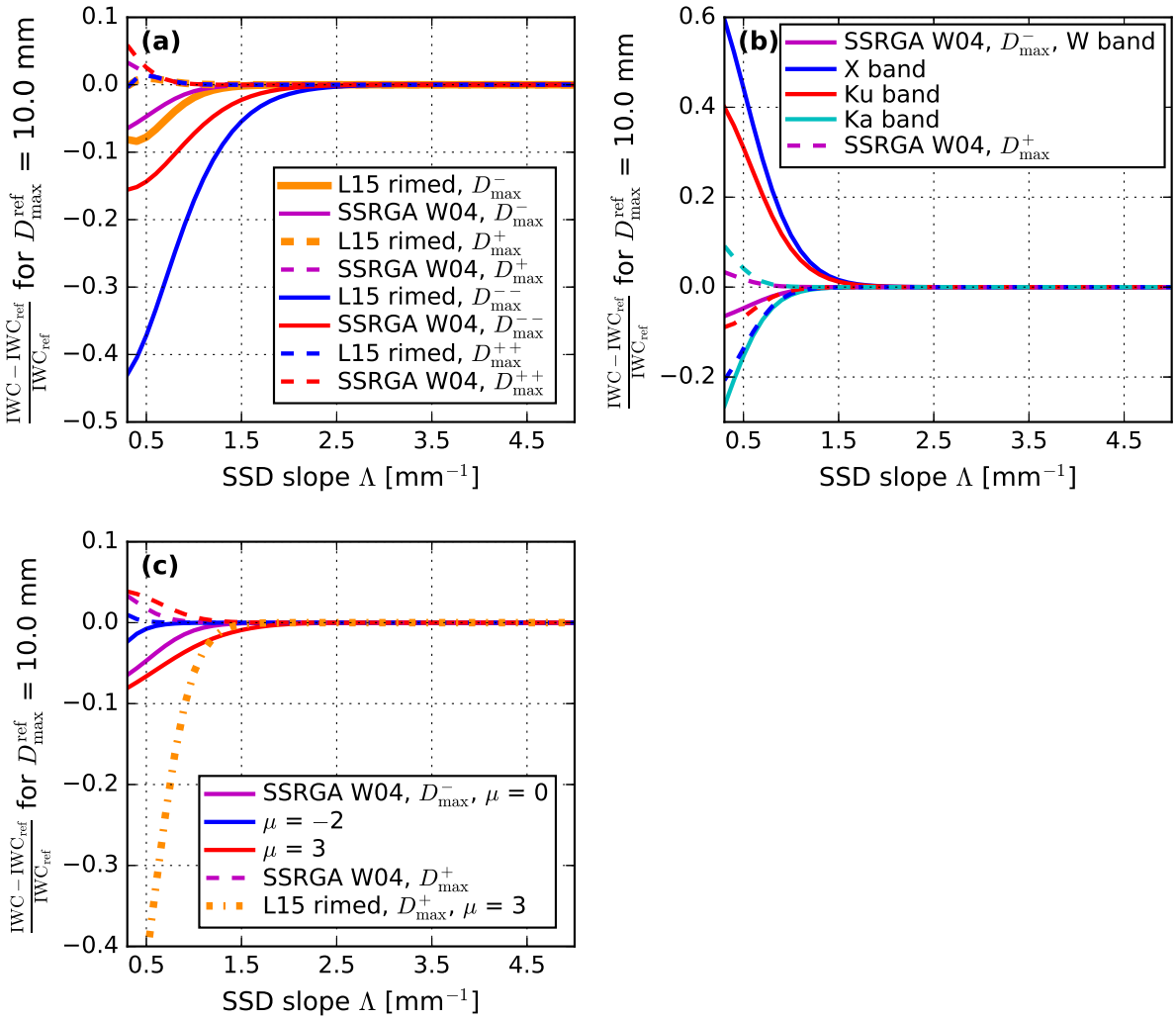

Figure S16: Impact of SSD cutoff size $D_{\max}$ on IWC retrievals as in Fig. 6 in the main article, but focusing on W band instead of Ku band: (a) W band, $\mu = 0$; (b) $\mu = 0$; (c) W band.

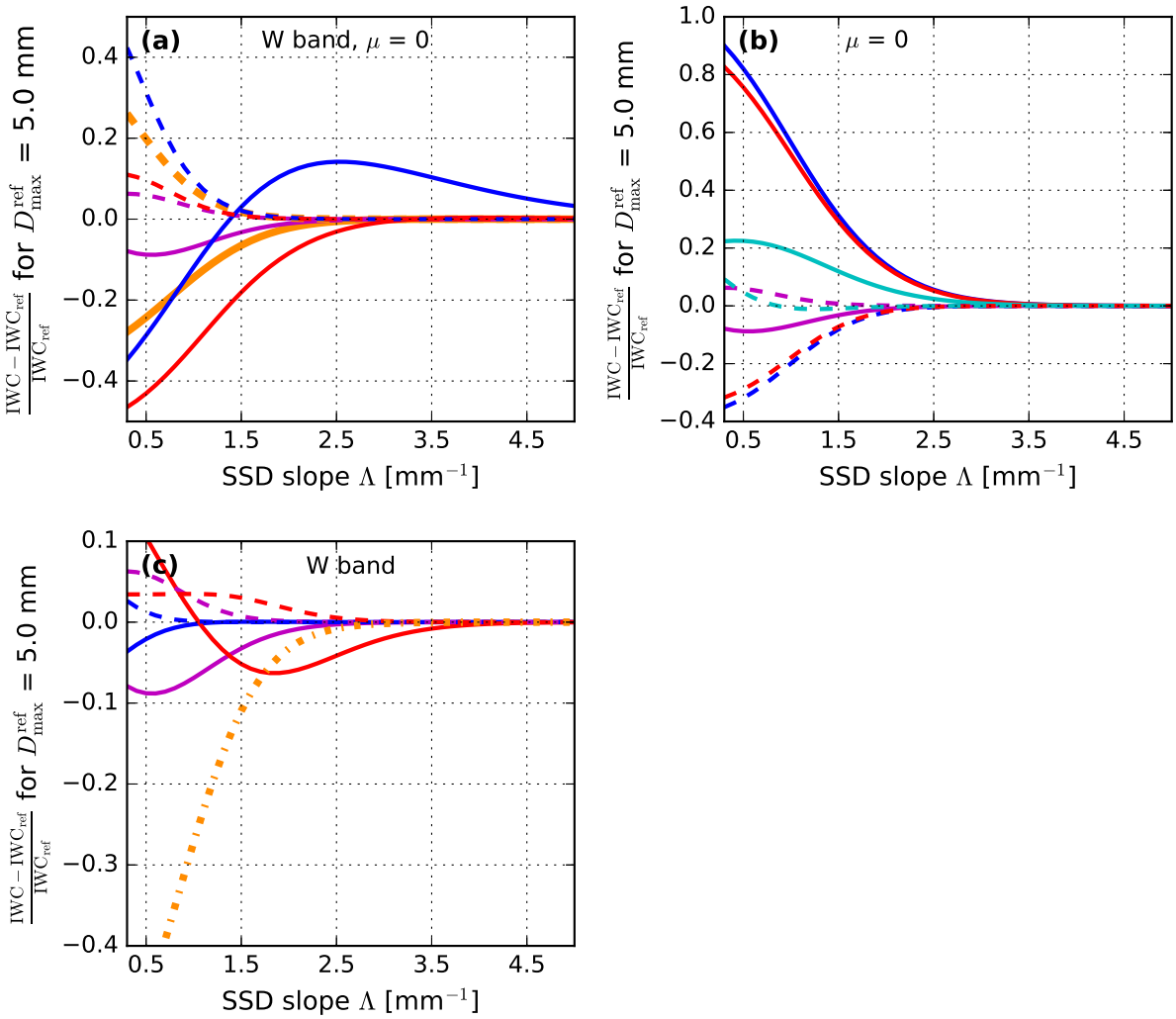

Figure S17: As Fig. S16, but for $D_{\mathrm{max}}^{\mathrm{ref}} = 5.0$ mm.

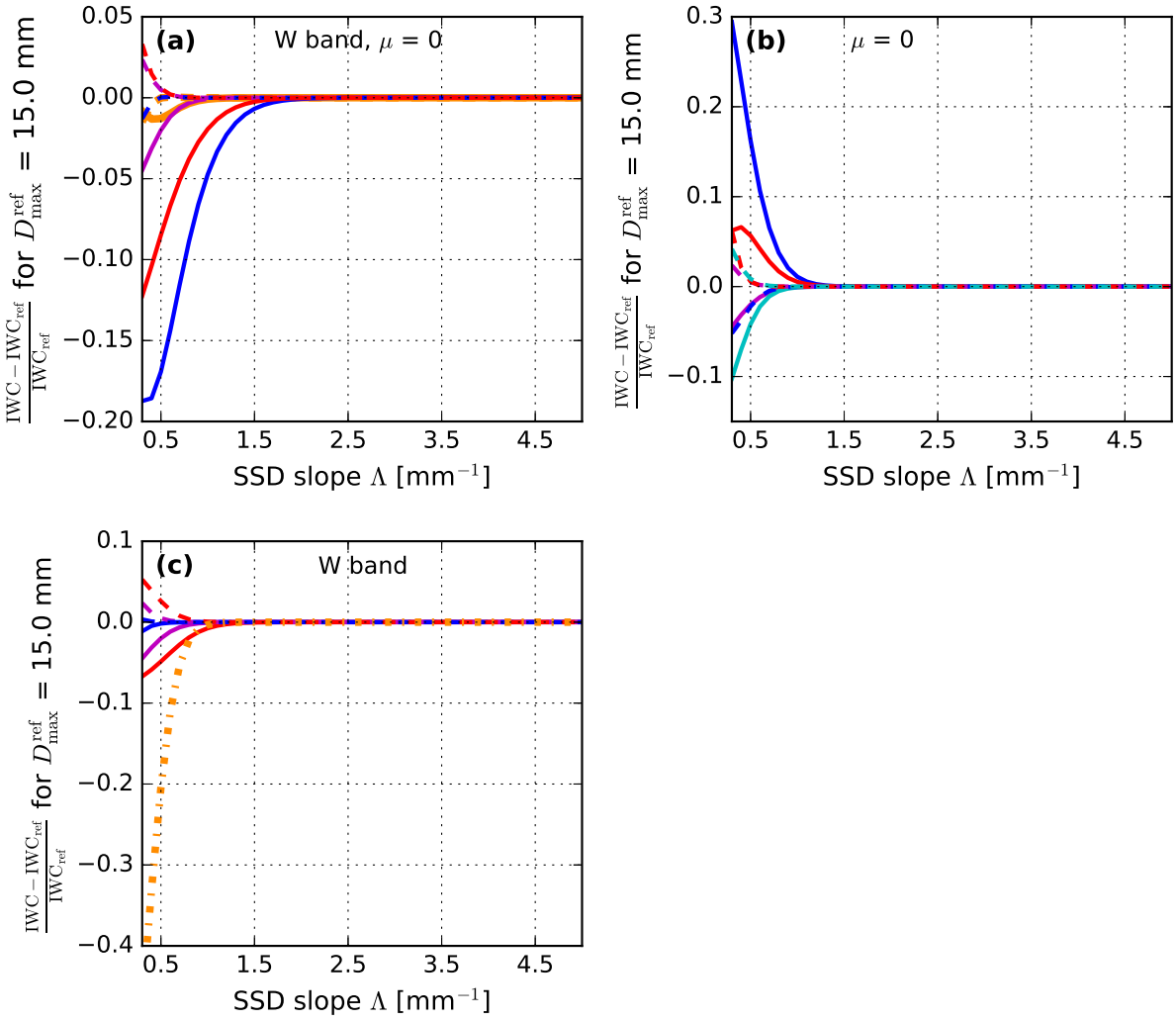

Figure S18: As Fig. S16, but for $D_{\mathrm{max}}^{\mathrm{ref}} = 15.0$ mm.

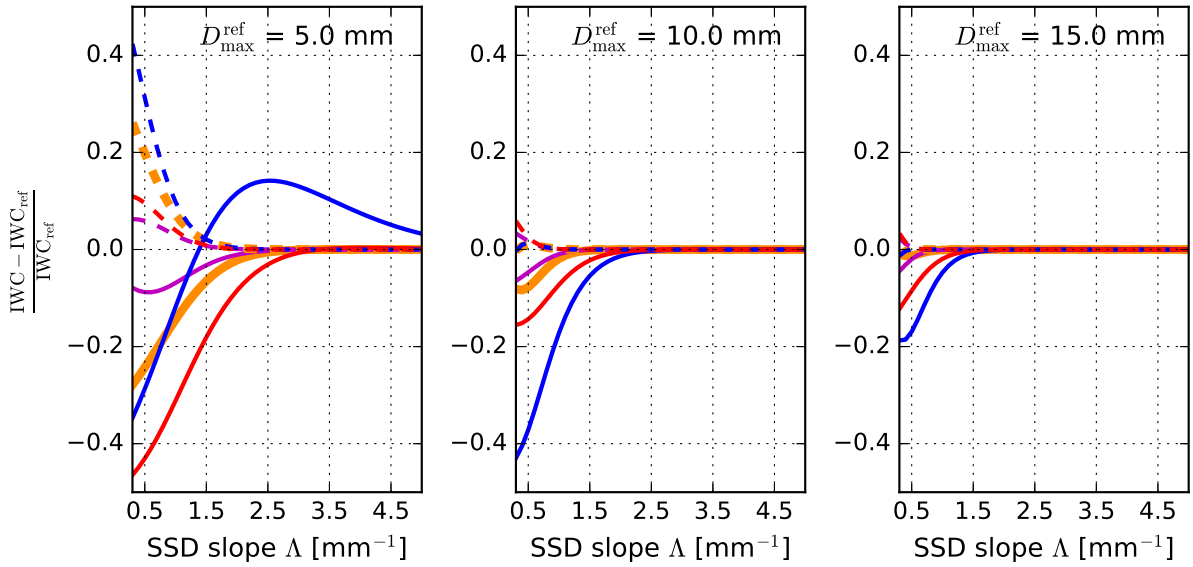

Figure S19: Impact of $D_{\max}$ on IWC retrievals for different $D_{\max}$ reference values of $D_{\max}^{\mathrm{ref}}$ = 5.0, 10.0, 15.0 mm as in Fig. 7 in the main article, but for W band instead of Ku band. See Fig. S16a for legend.

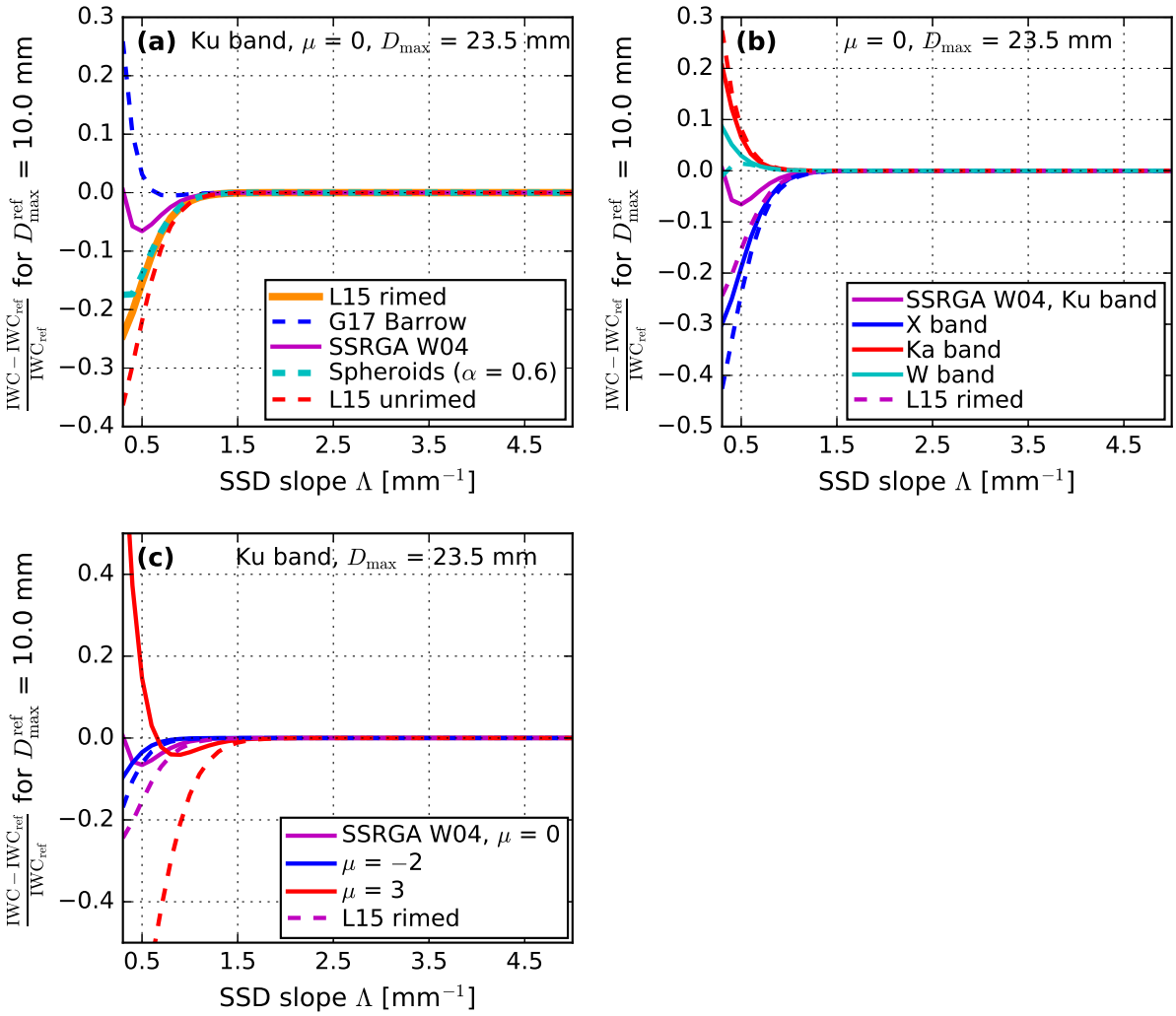

Figure S20: Impact of always assuming a maximum snowflake size of $D_{\max} = 23.5$ mm (for an actual maximum snowflake size of $D_{\max}^{\mathrm{ref}} = 10.0$ mm) on IWC retrievals.

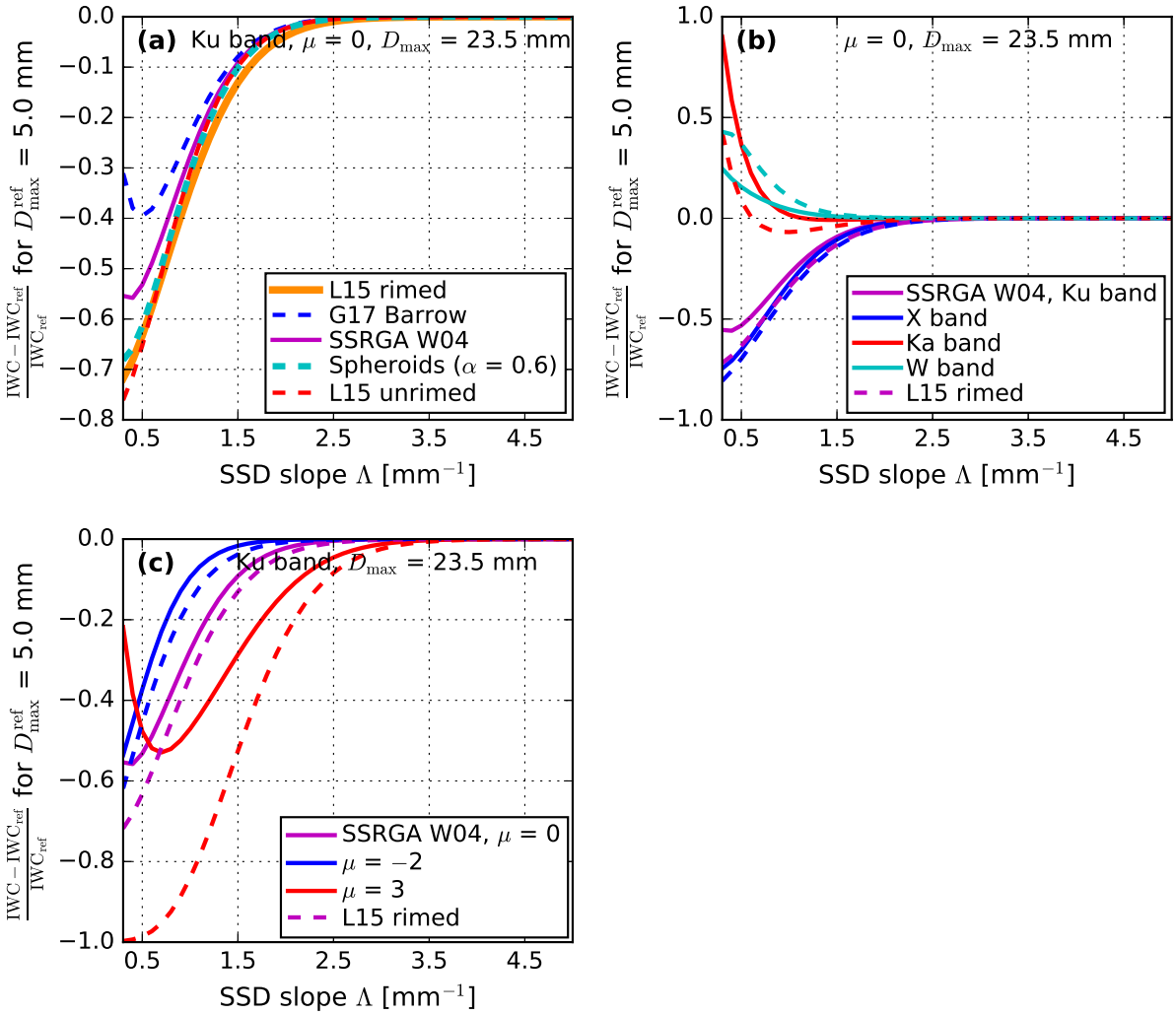

Figure S21: As Fig. S20, but for $D_{\max}^{\mathrm{ref}} = 5.0$ mm.

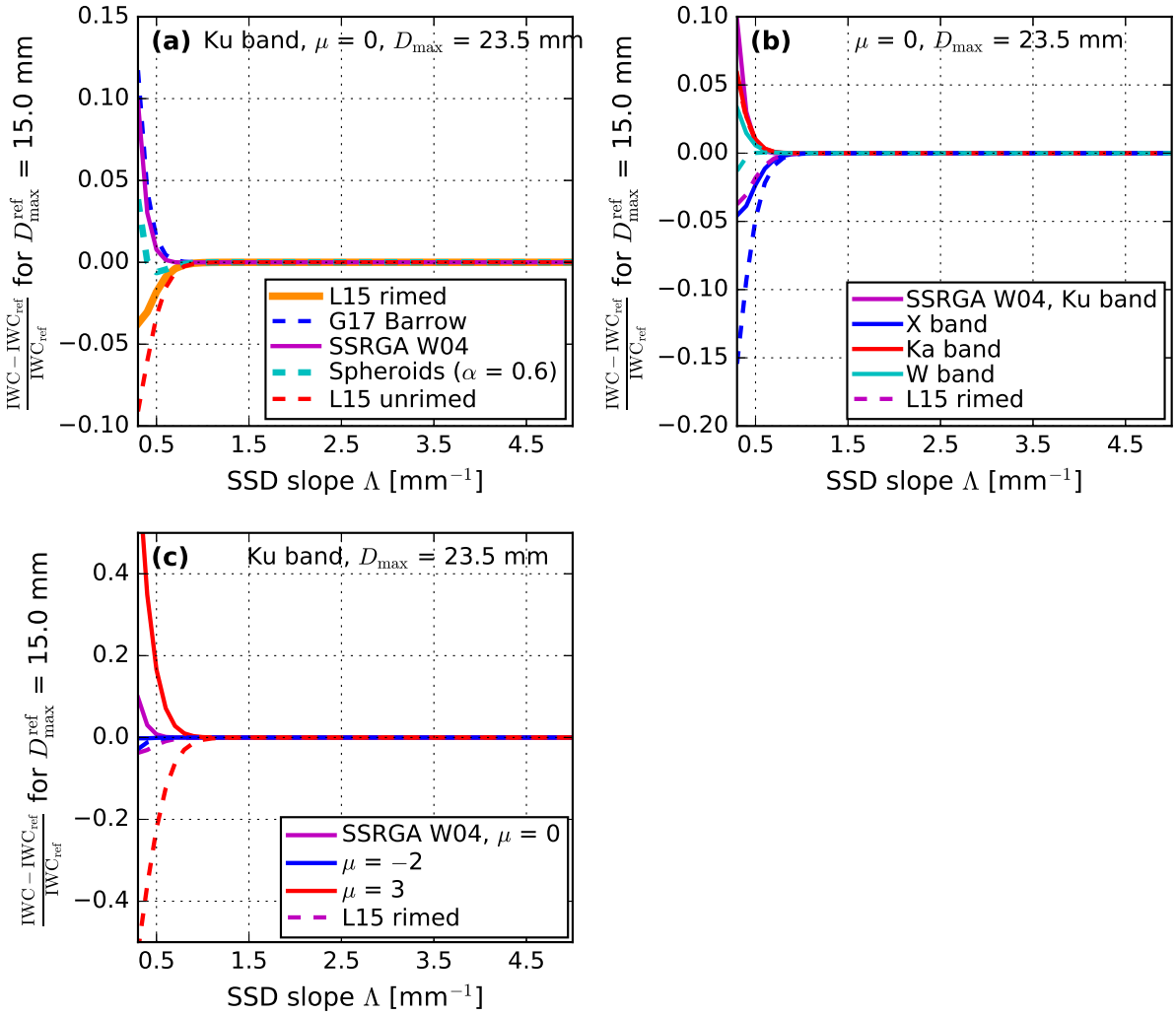

Figure S22: As Fig. S20, but for $D_{\max}^{\mathrm{ref}} = 15.0$ mm.

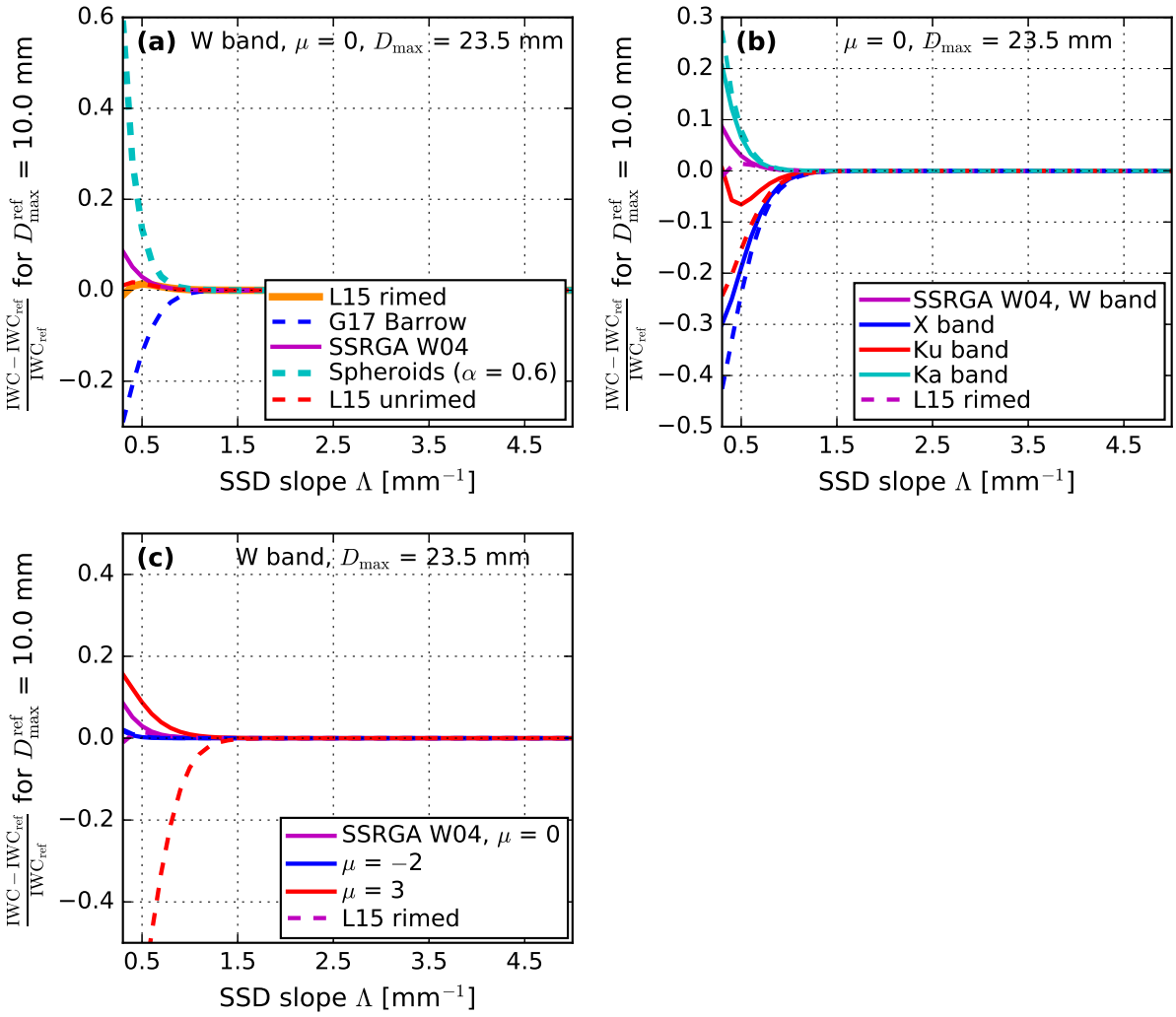

Figure S23: As Fig. S20, but focusing on W band instead of Ku band.

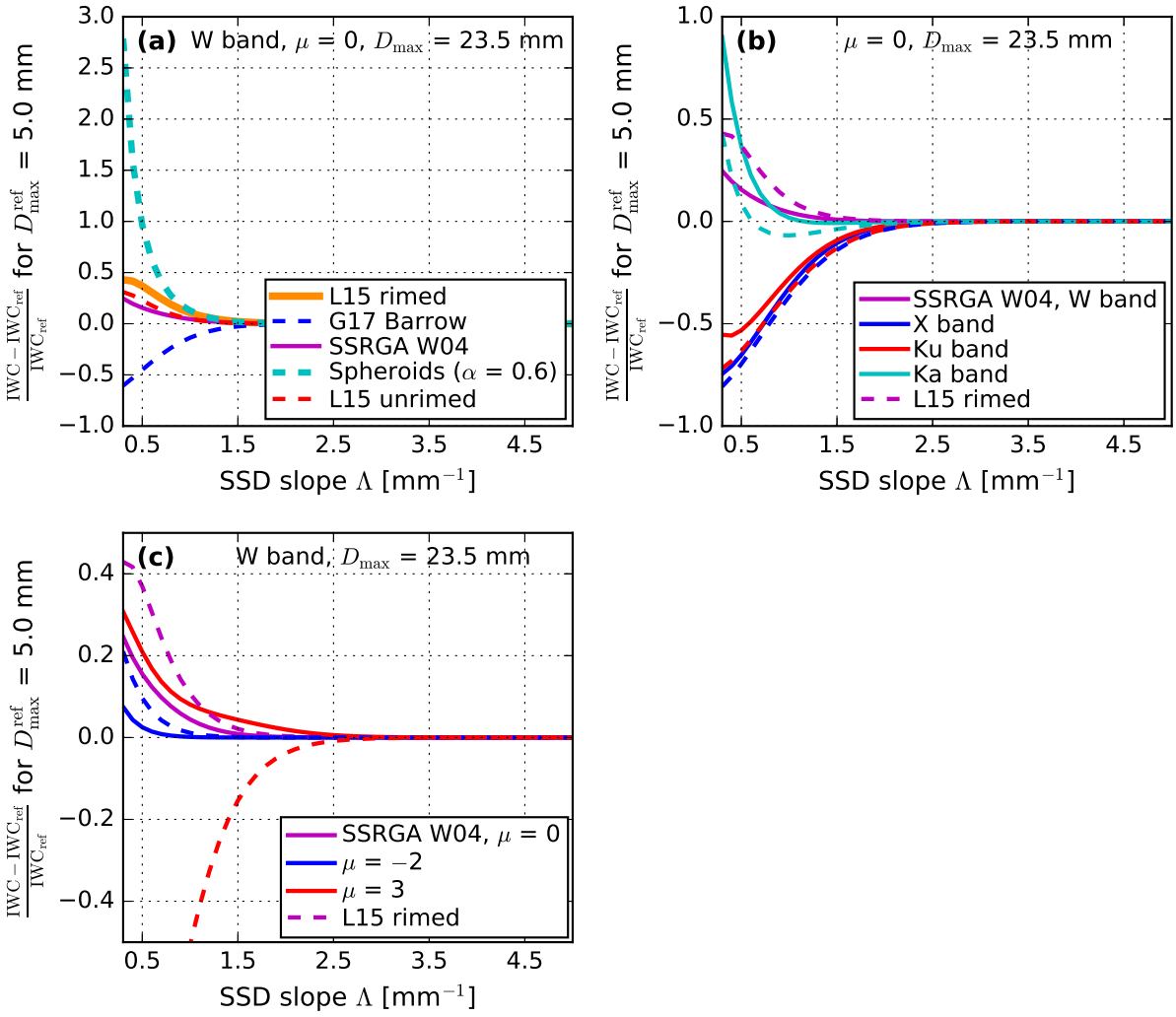

Figure S24: As Fig. S23, but for $D_{\max}^{\mathrm{ref}} = 5.0$ mm.

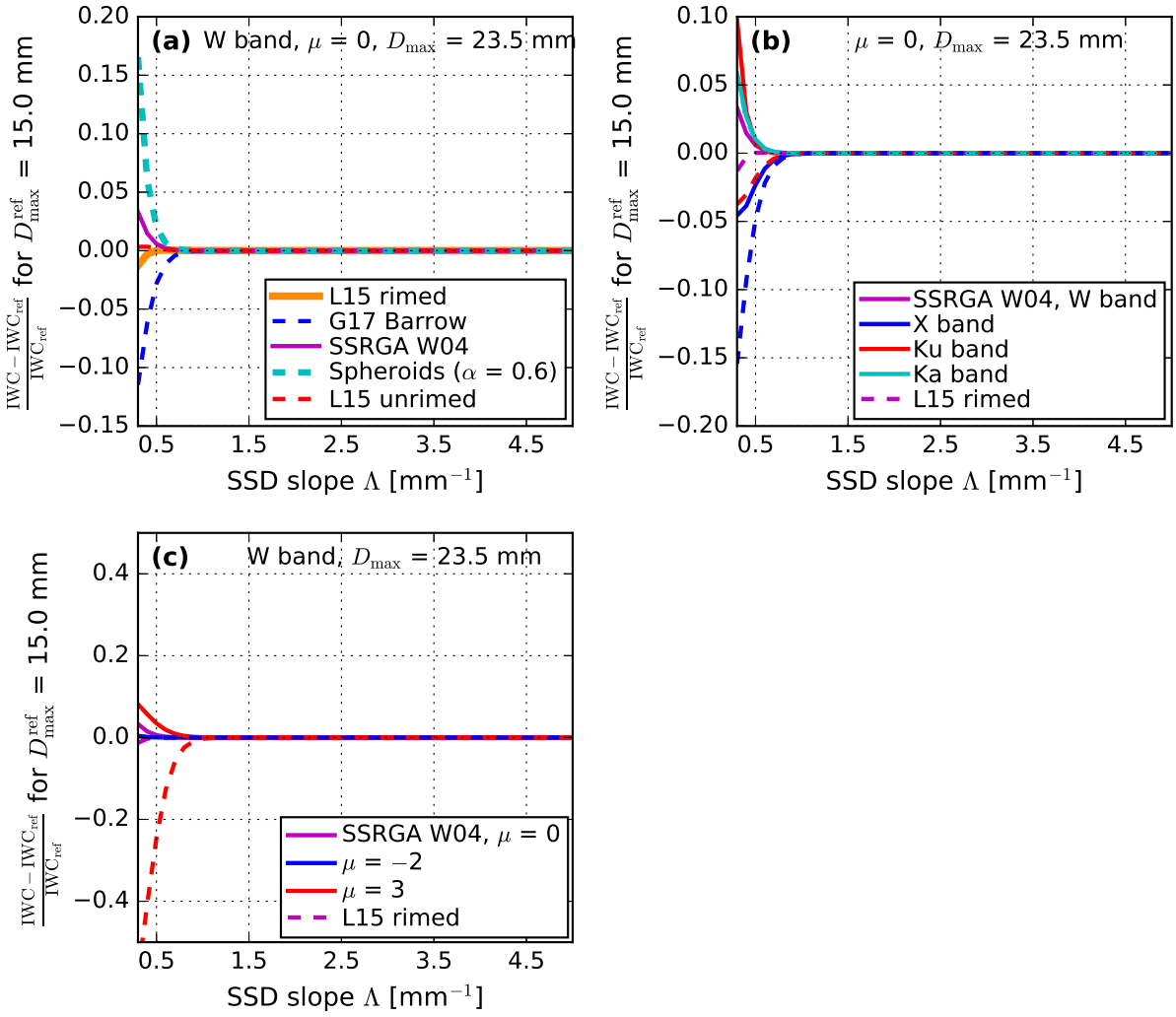

Figure S25: As Fig. S23, but for $D_{\max}^{\mathrm{ref}} = 15.0$ mm.

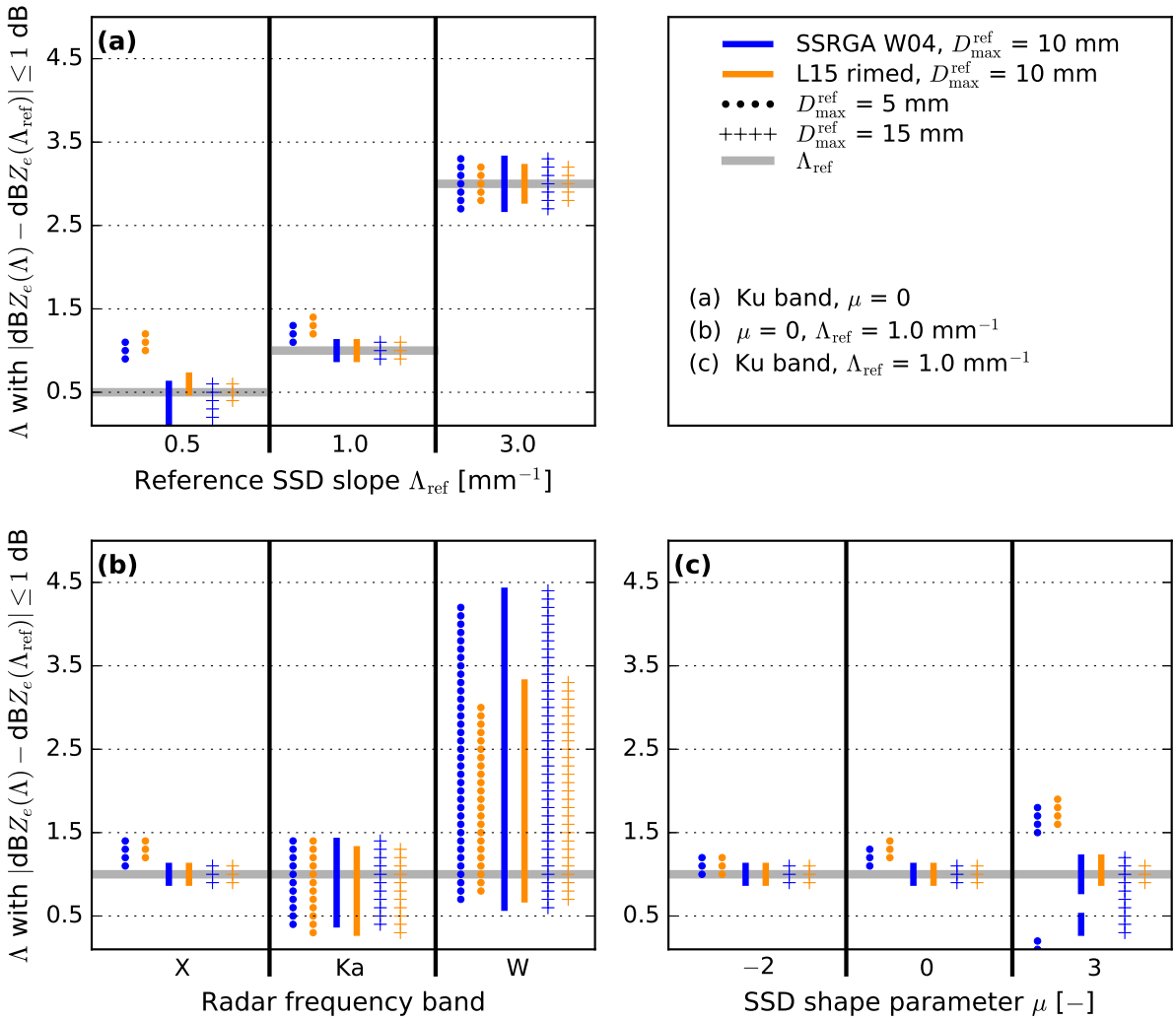

Figure S26: As Fig. 8 in the main article, but for always assuming a maximum snowflake size of $D_{\max} = 23.5$ mm (for an actual maximum snowflake size of $D_{\max}^{\mathrm{ref}}$ as indicated in the legend).

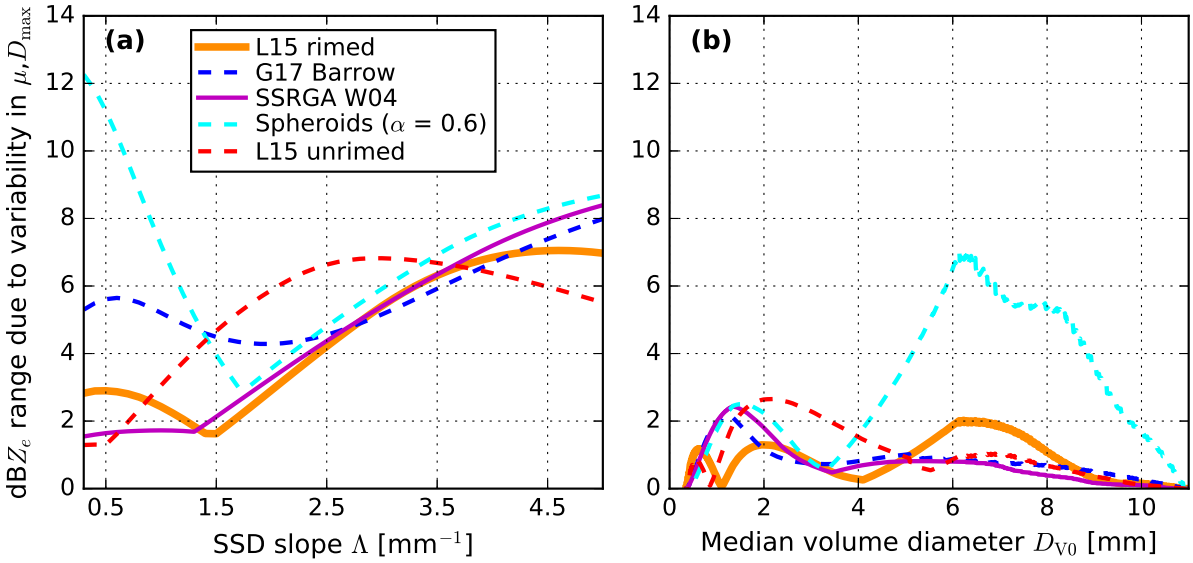

Figure S27: Effect of summarizing snowflake size distributions by the median volume diameter D_{V0} on the range of modeled radar reflectivity factors $\mathrm{dB}Z_e$ as in Fig. 10 in the main article, but for W band instead of Ku band.

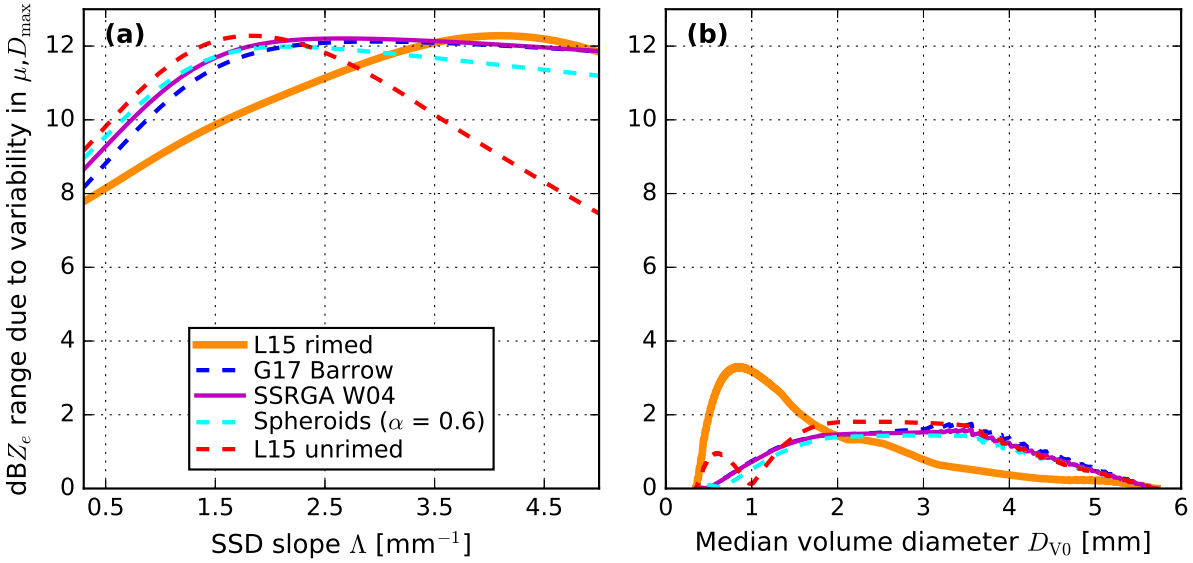

Figure S28: As Fig. 10 in the main article, but for a D_{max} reference value of $D_{\mathrm{max}}^{\mathrm{ref}} = 5.0$ mm.

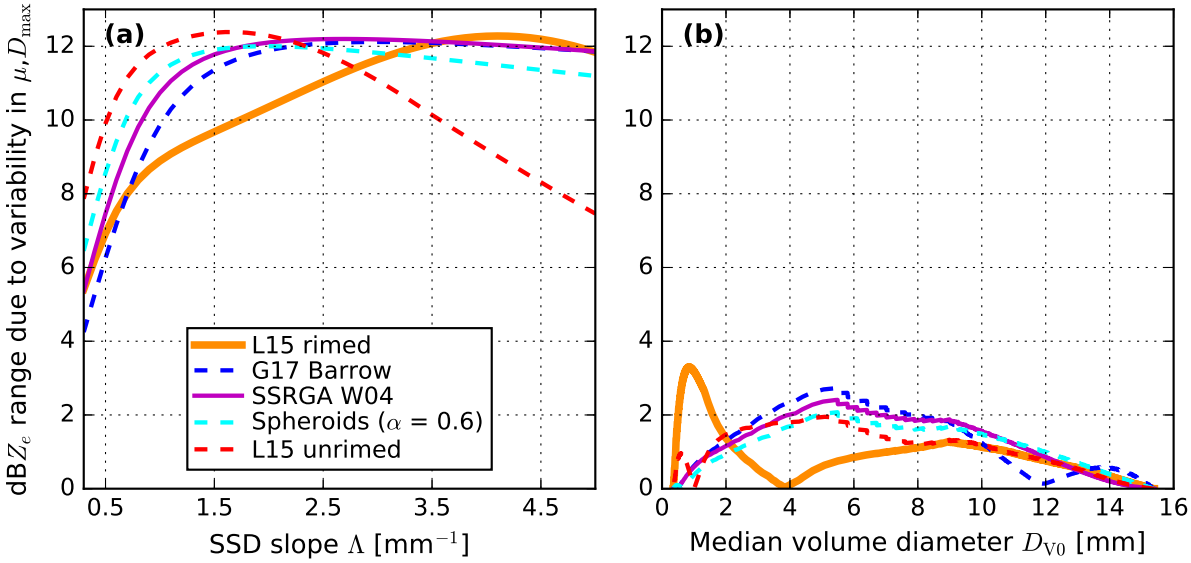

Figure S29: As Fig. 10 in the main article, but for a $D_{\max}$ reference value of $D_{\max}^{\text{ref}} = 15.0$ mm.

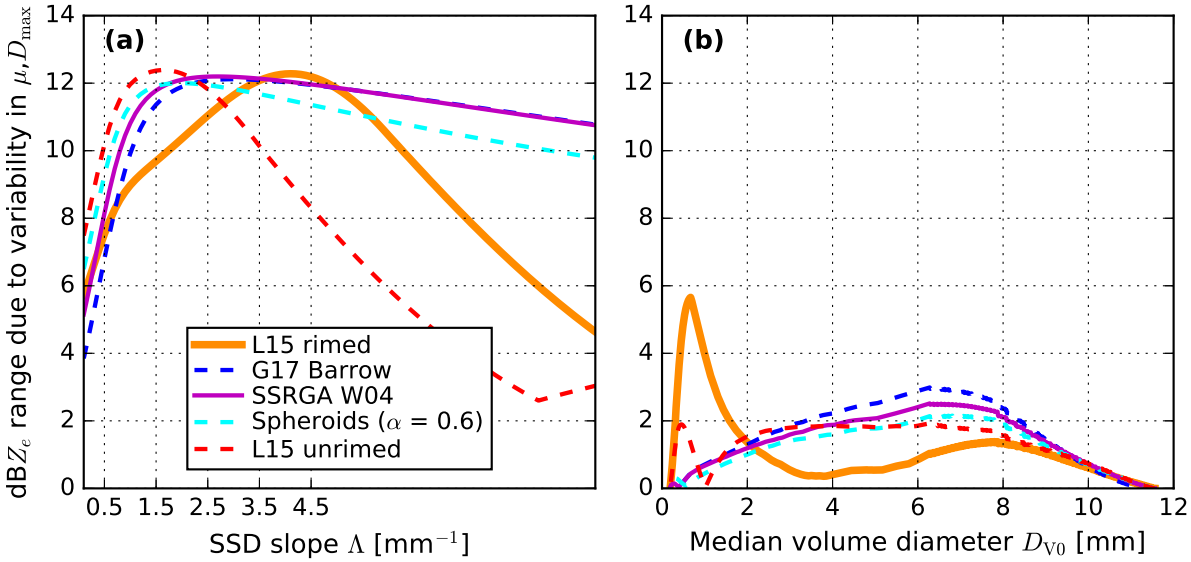

Figure S30: As Fig. 10 in the main article, but for a wider range of SSD slope parameters of $0.1 \leq \Lambda \leq 10.0$ mm^{-1}.

References

[1] T. J. Garrett, C. Fallgatter, K. Shkurko, D. Howlett, Fall speed measurement and high-resolution multi-angle photography of hydrometeors in free fall, Atmos. Meas. Tech. 5 (2012) 2625–2633. doi:10.5194/amt-5-2625-2012.

[2] M. Gergely, S. J. Cooper, T. J. Garrett, Using snowflake surface-area-to-volume ratio to model and interpret snowfall triple-frequency radar signatures, Atmos. Chem. Phys. 17 (2017) 12011–12030. doi:10.5194/acp-17-12011-2017.

[3] J. Leinonen, W. Szyrmer, Radar signatures of snowflake riming: A modeling study, Earth Space Sci. 2 (2015) 346–358. doi:10.1002/2015EA000102.

[4] R. J. Hogan, C. D. Westbrook, Equation for the microwave backscatter cross section of aggregate snowflakes using the self-similar Rayleigh–Gans approximation, J. Atmos. Sci. 71 (2014) 3292–3301. doi:10.1175/JAS-D-13-0347.1.

[5] R. J. Hogan, R. Honeyager, J. Tyynelä, S. Kneifel, Calculating the millimetre-wave scattering phase function of snowflakes using the self-similar Rayleigh–Gans Approximation, Q. J. R. Meteorol. Soc. 143 (2017) 834–844. doi:10.1002/qj.2968.

[6] C. D. Westbrook, R. C. Ball, P. R. Field, A. J. Heymsfield, Universality in snowflake aggregation, Geophys. Res. Lett. 31 (2004) L15104. doi:10.1029/2004GL020363.

[7] A. J. Heymsfield, A. Bansemer, C. Schmitt, C. Twohy, M. R. Poellot, Effective ice particle densities derived from aircraft data, J. Atmos. Sci. 61 (2004) 982–1003.